Ground-State Structure in $\nu = 2$ Bilayer Quantum Hall Systems

Z.F. Ezawa[1], M. Eliashvili[2] and G. Tsitsishvili[1,2]

[1]*Department of Physics, Tohoku University, Sendai, 980-8578 Japan   and*
[2]*Department of Theoretical Physics, A. Razmadze Mathematical Institute, Tbilisi, 380093 Georgia*
(Dated: February 2, 2008)

We investigate the ground-state structure of the bilayer quantum Hall system at the filling factor $\nu = 2$. Making an exact analysis of the ground state in the SU(4)-invariant limit, we include all other interactions as small perturbation. We carry out analytic calculations and construct phase diagrams for nonzero values of the Zeeman, tunneling and bias interactions. In particular we examine carefully how the phase transition occurs by applying the bias voltage and inducing a density imbalance between the two layers. We compare our theoretical result with the experimental data due to Sawada et al. based on the phase diagram in the σ_0-ρ_0 plane, where ρ_0 and σ_0 are the total electron density and the density difference between the two layers, respectively.

I. INTRODUCTION

A rich physics has emerged from the layer degree of freedom in the bilayer quantum Hall (QH) system[1,2]. An electron carries the SU(2) pseudospin index assigned to the front and back layers. The spin and the pseudospin are equal partners. There arises a unique phase at the filling factor $\nu = 1$. It is the spin-ferromagnet and pseudospin-ferromagnet phase, where various intralayer and interlayer coherent phenomena have been observed[1,2]. On the other hand, according to the one-body picture we expect to have two phases at $\nu = 2$ depending on the relative strength between the Zeeman gap Δ_Z and the tunneling gap Δ_{SAS}. One is the spin-ferromagnet and pseudospin-singlet phase (abridged as the spin phase[3]) for $\Delta_Z > \Delta_{SAS}$; the other is the spin-singlet and pseudospin-ferromagnet phase (abridged as the ppin phase[3]) for $\Delta_Z < \Delta_{SAS}$. Between these two phases, driven by interlayer correlations, a novel canted antiferromagnetic phase has been predicted to emerge[4,5].

The first experimental indication of a phase transition at $\nu = 2$ was revealed by inelastic light scattering spectroscopy[6]. An unambiguous evidence was subsequently obtained through magneto-transport measurements[7], where the importance of making density imbalance between the two layers is emphasized to study phase transitions. There is an attempt[8] to interpret the data[7] based on numerical analyses. However, the physical picture is not yet clear enough due to the lack of analytic understanding. For instance, it is yet to be explored how the density imbalance is induced as a function of the bias voltage V_{bias}. The density imbalance is made as soon as $V_{\text{bias}} \neq 0$ at $\nu = 1$, but this is not so simple at $\nu = 2$. Furthermore, the exact diagonalization[9] of a few-electron system has shown that the boundary between the spin and canted phases is practically unmodified but the boundary between the canted and ppin phases is considerably modified from the mean-field result. There is so far no theoretical explanation of these behaviors. The aim of this paper is to understand the ground-state structure of the $\nu = 2$ bilayer QH system more in details based on perturbation theory.

We investigate physics taking place in the lowest Landau level (LLL). Since each Landau site can accommodate four electrons with the spin and pseudospin degrees of freedom, the underlying group structure is enlarged to SU(4). We start with the SU(4)-invariant limit of the bilayer system, where the ground state is determined by solving the eigenvalue equation. We then include SU(4)-noninvariant terms perturbatively. The ground-state energy is calculated analytically in the first order of perturbation. Then we examine carefully how the phase transition occurs as the density imbalance is made between the two layers. We are particularly interested in the phase diagram in the σ_0-ρ_0 plane, where ρ_0 and σ_0 denotes the total electron density and the imbalance parameter (the normalized density difference between the two layers), respectively. This is because phase transition points have experimentally[7] been observed most clearly in such a plane. We also present the phase diagram in the the ρ_0-Δ_{SAS} plane, which will be useful to analyze experimental data obtained in samples with different Δ_{SAS} but all other parameters unchanged.

In Section II we review the Landau-site Hamiltonian governing bilayer QH systems[10]. In Section III we solve the eigenvalue equation for the ground state in the SU(4)-invariant limit. In so doing we identify the physical variables within 15 generators of the group SU(4). We show that there are 9 independent physical variables, among which 8 variables describe real Goldstone modes on the SU(4)-invariant ground state. We then calculate the ground-state energy of the full system in the first order of perturbation. In Section IV we verify the existence of the spin phase, the canted phase and the ppin phase in the presence of the bias voltage. The ground state is obtained in an analytic form in each phase. In particular the spin component S_z and the imbalance parameter σ_0 are calculated as functions of the bias voltage for typical sample parameters. In Section V we present phase diagrams in the Δ_{SAS}-Δ_Z plane, in the σ_0-ρ_0 plane and in the ρ_0-Δ_{SAS} plane. In Section VI we show that the spin phase is not modified but the ppin phase is considerably modified by higher order perturbations. Thus, the spin-canted phase boundary is an exact result, as is consistent with the result[9] obtained from the exact diagonalization of a few-electron system. In Section VII we interpret the

experimental data[7] based on the phase diagram in the σ_0-ρ_0 plane. Section VIII is devoted to discussions.

II. LANDAU-SITE HAMILTONIAN

Electrons in a plane perform cyclotron motion under strong magnetic field $B_\perp$ and create Landau levels. In QH systems the electron position is specified solely by the guiding center $\boldsymbol{X} = (X, Y)$ subject to the noncommutative relation, $[X, Y] = -i\ell_B^2$, with the magnetic length $\ell_B = \sqrt{\hbar/eB_\perp}$. It follows from this relation that each electron occupies an area $2\pi\ell_B^2$ labelled by the Landau-site index. The total number of Landaus sites is $N_\Phi = S/2\pi\ell_B^2 = N/\nu$, where N and S are the total electron number and the area of the system, respectively. Electrons behave as if they were on lattice sites, among which Coulomb interactions operate.

In the bilayer system an electron carries 4 different polarizations associated with the ordinary spin $(\uparrow, \downarrow)$ and two layers (f,b). These four polarizations can be incorporated in the isospin index $\mu =$f$\uparrow$, f$\downarrow$, b$\uparrow$, b$\downarrow$. In this notation the second quantized electron field in the lowest Landau level (LLL) appear as

$$\psi_\mu(\boldsymbol{x}) = \sum_{m=0}^{\infty} c_\mu(m)\langle \boldsymbol{x}|m\rangle, \qquad (2.1)$$

where $\langle \boldsymbol{x}|m\rangle$ is the one-body wave function for the Landau site $|m\rangle$ in the LLL with m labeling the angular momentum. The operators $c_\mu(m)$ and $c_\nu^\dagger(n)$ satisfy the standard anticommutation relations.

The electron field ψ_μ has four components, and the bilayer system possesses the underlying algebra SU(4). It has the subalgebra SU$_{\text{spin}}$(2)$\otimes$SU$_{\text{ppin}}$(2). We denote the 3 generators of the spin SU(2) algebra by τ_a^{spin}, and those of the pseudospin SU(2) generators by τ_a^{ppin}. There are remaining 9 generators in SU(4), which are given by $\tau_a^{\text{spin}}\tau_b^{\text{ppin}}$. Their properties are summarized as

$$\tau_a^{\text{spin}}\tau_b^{\text{spin}} = \delta_{ab}\mathbb{I} + i\varepsilon_{abc}\tau_c^{\text{spin}},$$
$$\tau_a^{\text{ppin}}\tau_b^{\text{ppin}} = \delta_{ab}\mathbb{I} + i\varepsilon_{abc}\tau_c^{\text{ppin}},$$
$$\tau_a^{\text{spin}}\tau_b^{\text{ppin}} = \tau_b^{\text{ppin}}\tau_a^{\text{spin}}, \qquad (2.2)$$

where $\mathbb{I}$ stands for the 4×4 identity matrix. Their explicit form is given in Appendix A.

All the physical operators required for the description of the system are constructed as bilinear combinations of $\psi(\boldsymbol{x})$ and $\psi^\dagger(\boldsymbol{x})$. They are 16 density operators

$$\rho(\boldsymbol{x}) = \psi^\dagger(\boldsymbol{x})\psi(\boldsymbol{x}),$$
$$S_a(\boldsymbol{x}) = \frac{1}{2}\psi^\dagger(\boldsymbol{x})\tau_a^{\text{spin}}\psi(\boldsymbol{x}),$$
$$P_a(\boldsymbol{x}) = \frac{1}{2}\psi^\dagger(\boldsymbol{x})\tau_a^{\text{ppin}}\psi(\boldsymbol{x}),$$
$$R_{ab}(\boldsymbol{x}) = \frac{1}{2}\psi^\dagger(\boldsymbol{x})\tau_a^{\text{spin}}\tau_b^{\text{ppin}}\psi(\boldsymbol{x}), \qquad (2.3)$$

where S_a describes the total spin, $2P_z$ measures the electron-density difference between the two layers. The operator R_{ab} transforms as a spin under SU$_{\text{spin}}$(2) and as a pseudospin under SU$_{\text{ppin}}$(2).

The total Hamiltonian consists of the Coulomb, Zeeman, tunneling and bias terms. The Coulomb interaction is decomposed into the SU(4)-invariant and SU(4)-noninvariant terms,

$$H_C^+ = \frac{1}{2}\int d^2x\,d^2y\,\rho(\boldsymbol{x})V^+(\boldsymbol{x}-\boldsymbol{y})\rho(\boldsymbol{y}),$$
$$H_C^- = 2\int d^2x\,d^2y\,P_z(\boldsymbol{x})V^-(\boldsymbol{x}-\boldsymbol{y})P_z(\boldsymbol{y}), \qquad (2.4)$$

where

$$V^\pm(\boldsymbol{x}) = \frac{e^2}{8\pi\varepsilon}\left(\frac{1}{|\boldsymbol{x}|} \pm \frac{1}{\sqrt{|\boldsymbol{x}|^2 + d^2}}\right) \qquad (2.5)$$

with d being the layer separation. The tunneling and bias terms are summarized into the pseudo-Zeeman term. Combining the Zeeman and pseudo-Zeeman terms we have

$$H_{\text{ZpZ}} = -\int d^2x\,\left(\Delta_{\text{Z}}S_z + \Delta_{\text{SAS}}P_x + \Delta_{\text{bias}}P_z\right), \qquad (2.6)$$

with the Zeeman gap Δ_{Z}, the tunneling gap Δ_{SAS} and the bias term $\Delta_{\text{bias}} = eV_{\text{bias}}$.

Substituting the field expansion (2.1) into $H_C^\pm$ we obtain Landau-site Hamiltonians[10],

$$H_C^+ = \sum_{mnij} V_{mnij}^+ \rho(m,n)\rho(i,j),$$
$$H_C^- = 4\sum_{mnij} V_{mnij}^- P_z(m,n)P_z(i,j), \qquad (2.7)$$

where the Coulomb matrix element is

$$V_{mnij}^\pm = \frac{1}{2}\int d^2x\,d^2y\,\langle m|\boldsymbol{x}\rangle\langle \boldsymbol{x}|n\rangle V^\pm(\boldsymbol{x}-\boldsymbol{y})\langle i|\boldsymbol{y}\rangle\langle \boldsymbol{y}|j\rangle, \qquad (2.8)$$

and

$$\rho(m,n) = \sum_\sigma c_\sigma^\dagger(m)c_\sigma(n),$$
$$S_a(m,n) = \frac{1}{2}\sum_{\sigma\tau} c_\sigma^\dagger(m)(\tau_a^{\text{spin}})_{\sigma\tau}c_\tau(n),$$
$$P_a(m,n) = \frac{1}{2}\sum_{\sigma\tau} c_\sigma^\dagger(m)(\tau_a^{\text{ppin}})_{\sigma\tau}c_\tau(n). \qquad (2.9)$$

They satisfy the W$_\infty$(4) algebra[10], which is the SU(4) extension of the W$_\infty$ algebra. The Zeeman and pseudo-Zeeman terms read

$$H_{\text{ZpZ}} = -\sum_n \left[\Delta_{\text{Z}}S_z(n,n) + \Delta_{\text{SAS}}P_x(n,n) + \Delta_{\text{bias}}P_z(n,n)\right]. \qquad (2.10)$$

The total Hamiltonian is $H = H_C^+ + H_C^- + H_{\text{ZpZ}}$.

III. PHYSICAL DEGREES OF FREEDOM

At $\nu = 2$ there are two electrons in one Landau site. We consider a creation operator of a pair of electrons at site n,

$$G^\dagger(n) = \frac{1}{2}\sum_{\mu\nu} g_{\mu\nu} c_\mu^\dagger(n)c_\nu^\dagger(n), \qquad (3.1)$$

where $g_{\mu\nu}$ is an antisymmetric complex matrix, $g_{\mu\nu} = -g_{\nu\mu}$. A homogeneous state is given by

$$|g\rangle = \prod_n G^\dagger(n)|0\rangle, \qquad (3.2)$$

when $g_{\mu\nu}$ is independent of the site index n. The normalization of the state, $\langle g|g\rangle = 1$, leads to

$$\mathrm{Tr}\left(gg^\dagger\right) = 2. \qquad (3.3)$$

Since $g_{\mu\nu}$ contains 6 independent complex parameters, there are 6 independent homogeneous states. They span the **6**-dimensional irreducible representation of SU(4)⊗SU(4).

It is hard to diagonalize the total Hamiltonian. Since we are interested in the regime where the SU(4)-invariant Coulomb term H_C^+ dominates all other interactions, we start with the ground state of the Hamiltonian H_C^+,

$$H_C^+|g\rangle = E_g^+|g\rangle. \qquad (3.4)$$

We include the SU(4)-noninvariant terms as small perturbation.

By requiring

$$\rho(m,n)|g\rangle = \nu\delta_{mn}|g\rangle, \qquad (3.5)$$

the eigenvalue equation (3.4) is satisfied with[10]

$$E_g^+ = -\nu\sum_{mn} V_{mnnm}^+ = -\nu\varepsilon_X^+ N_\Phi \qquad (3.6)$$

and

$$\varepsilon_X^\pm = \frac{1}{4}\sqrt{\frac{\pi}{2}}\left[1 \pm e^{\frac{1}{2}(d/\ell)^2}\mathrm{erfc}\left(\frac{d}{\sqrt{2}\ell}\right)\right]E_C^0. \qquad (3.7)$$

Here

$$E_C^0 = \frac{e^2}{4\pi\varepsilon\ell_B} \qquad (3.8)$$

is the Coulomb energy unit. Note that the direct energy part, $\nu^2\sum_{mi} V_{mmii}^+$, is cancelled out by the background neutralizing charge[10]. It is the ground state in the SU(4)-invariant limit of the system, which is the unperturbed system realized in the limits $d \to 0$, $\Delta_Z \to 0$, $\Delta_{SAS} \to 0$ and $\Delta_{bias} \to 0$.

We introduce the expectation value of isospin operators,

$$\mathcal{S}_a = \langle g|S_a(n,n)|g\rangle = \frac{1}{2}\mathrm{Tr}\left(\tau_a^{\mathrm{spin}}gg^\dagger\right),$$

$$\mathcal{P}_a = \langle g|P_a(n,n)|g\rangle = \frac{1}{2}\mathrm{Tr}\left(\tau_a^{\mathrm{ppin}}gg^\dagger\right),$$

$$\mathcal{R}_{ab} = \langle g|R_{ab}(n,n)|g\rangle = \frac{1}{2}\mathrm{Tr}\left(\tau_a^{\mathrm{spin}}\tau_b^{\mathrm{ppin}}gg^\dagger\right). \qquad (3.9)$$

They are the total spin per one Landau site, and so on. We pay a special attention to the imbalance parameter σ_0, which is the normalized density deference between the two layers, $|\sigma_0| \leq 1$. At $\nu = 2$ it is defined by

$$\sigma_0 \equiv \frac{\rho_f - \rho_b}{\rho_f + \rho_b} = \mathcal{P}_z. \qquad (3.10)$$

The relation (3.9) together with the normalization condition (3.3) yields

$$gg^\dagger = \frac{1}{2}\mathbb{I} + \frac{1}{2}\left(\tau_a^{\mathrm{spin}}\mathcal{S}_a + \tau_a^{\mathrm{ppin}}\mathcal{P}_a + \tau_a^{\mathrm{spin}}\tau_b^{\mathrm{ppin}}\mathcal{R}_{ab}\right). \qquad (3.11)$$

Here and hereafter the summation over repeated indices over the spin or the pseudospin is understood; for instance, $\mathbf{S}^2 = \mathcal{S}_a^2 = \sum_{a=xyz}\mathcal{S}_a\mathcal{S}_a$.

We study the condition (3.5). It holds trivially for $m = n$. The condition $\rho(m,n)|g\rangle = 0$ for $m \neq n$ yields

$$\sum_{\alpha\beta\mu\nu} g_{\alpha\beta}g_{\mu\nu} c_\alpha^\dagger(m)c_\beta^\dagger(m)c_\mu^\dagger(n)c_\nu^\dagger(n)|0\rangle = 0, \qquad (3.12)$$

which in turn leads to

$$\sum_{\alpha\beta\mu\nu} \epsilon_{\alpha\beta\mu\nu}g_{\alpha\beta}g_{\mu\nu} = 0, \qquad (3.13)$$

where $\epsilon_{\alpha\beta\mu\nu}$ is the totally antisymmetric tensor. It is equivalent to

$$\mathbf{S}^2 + \mathbf{\mathcal{P}}^2 + \mathbf{\mathcal{R}}^2 = 1, \qquad (3.14)$$

in terms of physical variables, as we verify in Appendix C.

It is interesting to note that the magnitude of the SU(4) isospin, $\mathbf{S}^2 + \mathbf{\mathcal{P}}^2 + \mathbf{\mathcal{R}}^2$, is fixed by the eigenvalue equation (3.4). Namely it is a dynamical variable. Indeed, we have

$$\mathbf{S}^2 + \mathbf{\mathcal{P}}^2 + \mathbf{\mathcal{R}}^2 = \cos^2 2\theta \qquad (3.15)$$

for the state

$$|g\rangle = \prod_n \left[\cos\theta\, c_{f\uparrow}^\dagger(n)c_{f\downarrow}^\dagger(n) + \sin\theta\, c_{b\uparrow}^\dagger(n)c_{b\downarrow}^\dagger(n)\right]|0\rangle. \qquad (3.16)$$

In general, we can only derive a kinematical constraint

$$\mathbf{S}^2 + \mathbf{\mathcal{P}}^2 + \mathbf{\mathcal{R}}^2 \leqslant 1 \qquad (3.17)$$

from their definition (3.9): See (B16) in Appendix B. This is in sharp contrast to the $\nu = 1$ case, where the

magnitude of the SU(4) isospin, $\mathbf{S}^2 + \mathbf{P}^2 + \mathbf{R}^2 = 3/4$, is fixed kinematically.

Though there are 12 real parameters in the antisymmetric matrix $g_{\mu\nu}$, one of them is unphysical for representing the overall phase, and another is fixed by the normalization condition (3.3). Then one variable is fixed by the condition (3.14) on the ground state $|g\rangle$. As we shall see soon [see (3.26)] and prove in Appendix C, there exists another unphysical variable which decouples on the ground state $|g\rangle$. Hence the parameter space characterizing the SU(4)-invariant ground state $|g\rangle$ contains 8 real independent variables. They are the 4 complex Goldstone modes associated with a spontaneous breakdown of the SU(4) symmetry in the SU(4)-invariant limit. The number of the Goldstone modes agrees with our previous result[11,12] obtained based on an effective theory with the use of composite bosons.

We now include the SU(4)-noninvariant interactions as small perturbation. The first order perturbation is to diagonalize the full Hamiltonian H within this subspace. Equivalently, the ground state is determined by minimizing the energy

$$E_{\mathrm{g}} \equiv \mathcal{E}_{\mathrm{g}} N_\Phi = \langle g|H|g\rangle \qquad (3.18)$$

within this parameter space. See Section VIII on this point.

It is straightforward to show that

$$\langle g|c_\mu^\dagger(m)c_\nu(n)|g\rangle = \delta_{mn}(gg^\dagger)_{\nu\mu}, \qquad (3.19)$$

and

$$\langle g|c_\mu^\dagger(m)c_\sigma^\dagger(i)c_\tau(j)c_\nu(n)|g\rangle$$
$$= \begin{cases} +\delta_{mn}g_{\mu\sigma}^\dagger g_{\nu\tau} & \text{for} \quad m=i, j=n \\ +\delta_{mn}\delta_{ij}(gg^\dagger)_{\tau\sigma}(gg^\dagger)_{\nu\mu} & \text{for} \quad m>i, j<n \\ -\delta_{mj}\delta_{in}(gg^\dagger)_{\nu\sigma}(gg^\dagger)_{\tau\mu} & \text{for} \quad m>i, j>n \\ -\delta_{mj}\delta_{in}(gg^\dagger)_{\nu\sigma}(gg^\dagger)_{\tau\mu} & \text{for} \quad m<i, j<n \\ +\delta_{mn}\delta_{ij}(gg^\dagger)_{\tau\sigma}(gg^\dagger)_{\nu\mu} & \text{for} \quad m<i, j>n \end{cases}$$
$$(3.20)$$

Thus

$$\frac{1}{N_\phi}\sum V_{mnij}^\pm \langle G|c_\mu^\dagger(m)c_\sigma^\dagger(i)c_\tau(j)c_\nu(n)|G\rangle$$
$$= (gg^\dagger)_{\tau\sigma}(gg^\dagger)_{\nu\mu}\varepsilon_{\mathrm{D}}^\pm - (gg^\dagger)_{\nu\sigma}(gg^\dagger)_{\tau\mu}\varepsilon_{\mathrm{X}}^\pm. \quad (3.21)$$

By using these formulas the ground-state energy per Landau site is calculated as

$$\mathcal{E}_{\mathrm{g}} = \varepsilon_{\mathrm{D}}^- \left[\mathrm{Tr}\left(\tau_z^{\mathrm{ppin}}gg^\dagger\right)\right]^2 - \varepsilon_{\mathrm{X}}^- \mathrm{Tr}\left(\tau_z^{\mathrm{ppin}}gg^\dagger\tau_z^{\mathrm{ppin}}gg^\dagger\right)$$
$$- \varepsilon_{\mathrm{X}}^+ \mathrm{Tr}\left(gg^\dagger gg^\dagger\right) - \frac{1}{2}\Delta_{\mathrm{Z}}\mathrm{Tr}\left(\tau_z^{\mathrm{spin}}gg^\dagger\right)$$
$$- \frac{1}{2}\Delta_{\mathrm{SAS}}\mathrm{Tr}\left(\tau_x^{\mathrm{ppin}}gg^\dagger\right) - \frac{1}{2}\Delta_{\mathrm{bias}}\mathrm{Tr}\left(\tau_z^{\mathrm{ppin}}gg^\dagger\right),$$
$$(3.22)$$

or

$$\mathcal{E}_{\mathrm{g}} = 4\varepsilon_{\mathrm{D}}^- \mathcal{P}_z^2 - \left(\varepsilon_{\mathrm{X}}^+ - \varepsilon_{\mathrm{X}}^-\right)\left(\mathcal{S}_a^2 + \mathcal{P}_a^2 + \mathcal{R}_{ab}^2\right)$$
$$- 2\varepsilon_{\mathrm{X}}^-\left(\mathcal{S}_a^2 + \mathcal{P}_z^2 + \mathcal{R}_{az}^2\right) - \varepsilon_{\mathrm{X}}^+ - \varepsilon_{\mathrm{X}}^-$$
$$- \Delta_{\mathrm{Z}}\mathcal{S}_z - \Delta_{\mathrm{SAS}}\mathcal{P}_x - \Delta_{\mathrm{bias}}\mathcal{P}_z, \qquad (3.23)$$

where $\varepsilon_X^\pm$ is given by (3.7) and

$$\varepsilon_{\mathrm{D}}^- = \frac{1}{4}\frac{d}{\ell}E_{\mathrm{C}}^0. \qquad (3.24)$$

It is necessary to express 15 isospin components, $\mathcal{S}_a$, $\mathcal{P}_a$ and $\mathcal{R}_{ab}$ in terms of independent variables.

We may choose $\mathcal{S}_a$ and $\mathcal{P}_a$ as 6 independent variables. We expect that $\mathcal{R}_{ab}$ are written in terms of these 6 variables and 4 extra variables. Indeed, as demonstrated in the Appendix A, we obtain

$$\mathcal{R}_{ab} = \frac{\mathbf{S}^2\mathcal{P}_a - (\mathbf{SP})\mathcal{S}_a}{\mathcal{SQ}}\frac{\mathbf{P}^2\mathcal{S}_b - (\mathbf{SP})\mathcal{P}_b}{\mathcal{PQ}}\mathcal{R}_{PS}$$
$$+ \frac{\mathbf{S}^2\mathcal{P}_a - (\mathbf{SP})\mathcal{S}_a}{\mathcal{SQ}}\frac{\mathcal{Q}_b}{\mathcal{Q}}\mathcal{R}_{PQ}$$
$$+ \frac{\mathcal{Q}_a}{\mathcal{Q}}\frac{\mathbf{P}^2\mathcal{S}_b - (\mathbf{SP})\mathcal{P}_b}{\mathcal{PQ}}\mathcal{R}_{QS} + \frac{\mathcal{Q}_a}{\mathcal{Q}}\frac{\mathcal{Q}_b}{\mathcal{Q}}\mathcal{R}_{QQ} \qquad (3.25)$$

with $\mathcal{Q}_a \equiv \varepsilon_{abc}\mathcal{S}_b\mathcal{P}_c$, $\mathcal{S} = |\mathbf{S}|$, $\mathcal{P} = |\mathbf{P}|$ and $\mathcal{Q} = |\mathbf{Q}|$. Here, $\mathcal{R}_{PS}$, $\mathcal{R}_{PQ}$, $\mathcal{R}_{QS}$ and $\mathcal{R}_{QQ}$ are the 4 extra variables. However, it can be proved that only 3 of them are independent, and they are parametrized as

$$\mathcal{R}_{PS} + i\mathcal{R}_{QS} = e^{i\omega}\left(-i\lambda + \frac{1}{\xi}\mathcal{S}\right),$$
$$\mathcal{R}_{PQ} + i\mathcal{R}_{QQ} = -ie^{i\omega}\xi\mathcal{P}. \qquad (3.26)$$

Thus $\mathcal{R}_{ab}$ are expressed in terms of 9 variables; ξ, λ, ω together with $\mathcal{S}_a$, $\mathcal{P}_a$. One variable is unexpectedly unphysical, about which we explain in Appendix B.

We show that $\mathcal{S}_x = \mathcal{S}_y = \mathcal{P}_y = 0$ for the ground state. First of all $\mathcal{S}_a$ and $\mathcal{R}_{az}$ rotate as vectors under the $\mathrm{SU}_{\mathrm{spin}}(2)$ transformation. So, if we have any configuration with nonvanishing $\mathcal{S}_x$ and $\mathcal{S}_y$, we can perform an $\mathrm{SU}_{\mathrm{spin}}(2)$ rotation to increase $\mathcal{S}_z$, without affecting $\mathcal{S}_a^2$ and $\mathcal{R}_{az}^2$, as far as possible until $\mathcal{S}_x = \mathcal{S}_y = 0$. This decreases the energy (3.23). Similarly, performing an $\mathrm{SU}_{\mathrm{ppin}}(2)$ rotation in the xy-pseudoplane, we can lower the energy via the tunneling term by increasing $\mathcal{P}_x$, without affecting $\mathcal{P}_z$ and $\mathcal{R}_{az}^2$, as far as possible until $\mathcal{P}_y = 0$.

Substituting $\mathcal{S}_x = \mathcal{S}_y = \mathcal{P}_y = 0$ into R_{ab} we come to

$$\sum_{ab}\mathcal{R}_{ab}^2 = \frac{\mathcal{S}_z^2}{\xi^2} + \lambda^2 + \xi^2\left(\mathcal{P}_x^2 + \mathcal{P}_z^2\right),$$
$$\sum_a\mathcal{R}_{az}^2 = \left(\frac{\mathcal{S}_z^2}{\xi^2} + \lambda^2\right)\frac{\mathcal{P}_x^2}{\mathcal{P}_x^2 + \mathcal{P}_z^2}. \qquad (3.27)$$

Hence the energy (3.23) yields

$$\mathcal{E}_{\mathrm{g}} = \left(\varepsilon_{\mathrm{X}}^- - \varepsilon_{\mathrm{X}}^+\right)\left[\left(1 + \frac{1}{\xi^2}\right)\mathcal{S}_z^2 + \left(\mathcal{P}_x^2 + \mathcal{P}_z^2\right)\left(1 + \xi^2\right)\right]$$
$$- 2\varepsilon_{\mathrm{X}}^-\mathcal{S}_z^2 + \varepsilon_{\mathrm{cap}}\mathcal{P}_z^2 - 2\varepsilon_{\mathrm{X}}^-\frac{\mathcal{P}_x^2}{\mathcal{P}_x^2 + \mathcal{P}_z^2}\frac{\mathcal{S}_z^2}{\xi^2}$$
$$- \varepsilon_{\mathrm{X}}^+ - \varepsilon_{\mathrm{X}}^- - \Delta_{\mathrm{Z}}\mathcal{S}_z - \Delta_{\mathrm{SAS}}\mathcal{P}_x - \Delta_{\mathrm{bias}}\mathcal{P}_z$$
$$- \left(\varepsilon_{\mathrm{X}}^+ - \varepsilon_{\mathrm{X}}^- + 2\varepsilon_{\mathrm{X}}^-\frac{\mathcal{P}_x^2}{\mathcal{P}_x^2 + \mathcal{P}_z^2}\right)\lambda^2, \qquad (3.28)$$

where we have set

$$\varepsilon_{\text{cap}} \equiv 4\varepsilon_D^- - 2\varepsilon_X^-. \qquad (3.29)$$

Here $\varepsilon_{\text{cap}}\mathcal{P}_z^2$ is the capacitance energy per one Landau site. The capacitance parameter (3.29) is different from the $\nu = 1$ QH system[10], where $\varepsilon_{\text{cap}}^{\nu=1} \equiv 4\varepsilon_D^- - 4\varepsilon_X^-$. Note that the energy formula (3.23) holds as it stands also at $\nu = 1$. The difference arises because $\sum_a \mathcal{R}_{az}^2 = \mathcal{P}_z^2$ in (3.23) at $\nu = 1$ but it is given by (3.27) at $\nu = 2$.

If we minimize $\mathcal{E}_g$ within the parameter space of the SU(4)-invariant ground state, we should impose the condition (3.14). However, it is instructive to minimize $\mathcal{E}_g$ without requiring it. Namely, we only assume the kinematical condition (3.17), which reads

$$\left(1 + \frac{1}{\xi^2}\right)\mathcal{S}_z^2 + \left(\mathcal{P}_x^2 + \mathcal{P}_z^2\right)\left(1 + \xi^2\right) + \lambda^2 \leq 1. \quad (3.30)$$

Nevertheless, the equality is easily seen to hold on the minimum-energy state. Indeed, let us assume that it is realized with the inequality. However, this is self-contradictory since we can decrease the energy $\mathcal{E}_g$ by increasing λ^2 in (3.28) as far as the inequality is obeyed; note that $\varepsilon_X^+ > \varepsilon_X^-$. The self-contradiction is resolved only if the equality holds in (3.30),

$$\left(1 + \frac{1}{\xi^2}\right)\mathcal{S}_z^2 + \left(\mathcal{P}_x^2 + \mathcal{P}_z^2\right)\left(1 + \xi^2\right) + \lambda^2 = 1. \quad (3.31)$$

Namely, even if we minimize the energy $\mathcal{E}_g$ without imposing (3.14), we reproduce it. Consequently, the variation approach reproduces the ground-state condition (3.5) within the class of test functions (3.2).

We note that ω disappears both from (3.28) and (3.30), and hence it is a zero-energy mode even in the SU(4)-noninvariant case. We shall see that it is related with the rotational invariance in the xy-plane: See (4.3).

We eliminate λ^2 in (3.28) by using (3.31),

$$\begin{aligned}\mathcal{E}_g =&\, 2\varepsilon_X^- \frac{\mathcal{P}_z^2}{\mathcal{P}_x^2 + \mathcal{P}_z^2}\left(1 - \mathcal{S}_z^2\right) + 2\varepsilon_X^-\left(1 + \xi^2\right)\mathcal{P}_x^2 \\ &+ \varepsilon_{\text{cap}}\mathcal{P}_z^2 - \Delta_Z\mathcal{S}_z - \Delta_{\text{SAS}}\mathcal{P}_x - \Delta_{\text{bias}}\mathcal{P}_z \\ &- 2\varepsilon_X^+ - 2\varepsilon_X^-. \end{aligned} \qquad (3.32)$$

It is clear that we can decrease the energy by increasing $\mathcal{S}_z$ without affecting other terms in (3.32). This is achieved at by decreasing λ^2 until $\lambda^2 = 0$ in (3.31), which yields

$$\mathcal{S}_z^2 + \xi^2\left(\mathcal{P}_x^2 + \mathcal{P}_z^2\right) = \frac{\xi^2}{1 + \xi^2}. \qquad (3.33)$$

We solve this as

$$\begin{aligned}\mathcal{S}_z &= \frac{\xi}{\sqrt{1 + \xi^2}}\sqrt{1 - \alpha^2}, \\ \mathcal{P}_x &= \frac{1}{\sqrt{1 + \xi^2}}\alpha\sqrt{1 - \beta^2}, \\ \mathcal{P}_z &= \frac{1}{\sqrt{1 + \xi^2}}\alpha\beta \end{aligned} \qquad (3.34)$$

in terms of two parameters $|\alpha| \leq 1$ and $|\beta| \leq 1$.

Substituting these into (3.32) we obtain

$$\begin{aligned}\mathcal{E}_g =&\, 2\varepsilon_X^-\alpha^2 + \left[2\varepsilon_X^- + 4\left(\varepsilon_D^- - \varepsilon_X^-\right)\alpha^2\right]\frac{\beta^2}{1 + \xi^2} \\ &- \frac{\Delta_Z\xi}{\sqrt{1 + \xi^2}}\sqrt{1 - \alpha^2} - \frac{\Delta_{\text{SAS}}}{\sqrt{1 + \xi^2}}\alpha\sqrt{1 - \beta^2} \\ &- \frac{\Delta_{\text{bias}}}{\sqrt{1 + \xi^2}}\alpha\beta - 2\varepsilon_X^+ - 2\varepsilon_X^-. \end{aligned} \qquad (3.35)$$

To minimize this with respect to α, β and ξ, we write down the equations $\partial_\alpha E = \partial_\beta E = \partial_\xi E = 0$. We rearrange them as

$$\Delta_Z^2 = \frac{\Delta_{\text{SAS}}^2}{1 - \beta^2} - \frac{4\varepsilon_X^-\left(\Delta_0^2 - \beta^2\Delta_{\text{SAS}}^2\right)}{\Delta_0\sqrt{1 - \beta^2}}, \qquad (3.36a)$$

$$\frac{\Delta_{\text{bias}}}{\beta\Delta_{\text{SAS}}} = \frac{4\left(\varepsilon_X^- + 2\alpha^2\left(\varepsilon_D^- - \varepsilon_X^-\right)\right)}{\Delta_0} + \frac{1}{\sqrt{1 - \beta^2}}, \quad (3.36b)$$

$$\xi = \frac{\Delta_Z}{\Delta_{\text{SAS}}}\frac{\sqrt{1 - \alpha^2}}{\alpha}\sqrt{1 - \beta^2}, \qquad (3.36c)$$

where

$$\Delta_0 \equiv \sqrt{\Delta_{\text{SAS}}^2\alpha^2 + \Delta_Z^2\left(1 - \alpha^2\right)\left(1 - \beta^2\right)}. \qquad (3.37)$$

The ground state is determined by these equations. The parameters α and β are solved out from (3.36a) and (3.36b) in terms of the sample parameters [FIG.1]. Then, ξ is given by (3.36c) in terms of them.
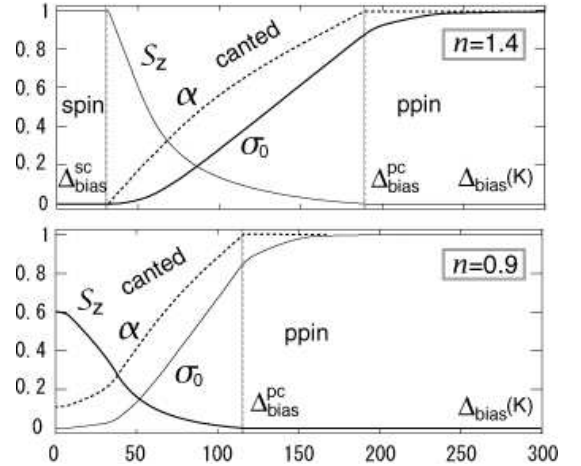

FIG. 1: The spin component $\mathcal{S}_z$ and the imbalance parameter $\sigma_0 \equiv \mathcal{P}_z$ are illustrated together with α as functions of Δ_{bias} for typical sample parameters ($d = 23\text{nm}$, $\Delta_{\text{SAS}} = 6.7\text{K}$ and $\rho_0 = n \times 10^{11}/\text{cm}^2$). The spin phase ($\alpha = 0$), the canted phase ($0 < \alpha < 1$) and the ppin phase ($\alpha = 1$) are realized for $\Delta_{\text{bias}} < \Delta_{\text{bias}}^{\text{sc}}$, $\Delta_{\text{bias}}^{\text{sc}} < \Delta_{\text{bias}} < \Delta_{\text{bias}}^{\text{pc}}$ and $\Delta_{\text{bias}}^{\text{pc}} < \Delta_{\text{bias}}$, respectively. There are 3 phases for $n = 1.4$ but only 2 phases for $n = 0.9$.

IV. GROUND-STATE STRUCTURE

We discuss the ground-state structure as a function of parameters α and β. Substituting (3.36c) into (3.34) we get

$$
\begin{aligned}
\mathcal{S}_z &= \frac{\Delta_{\mathrm{Z}}}{\Delta_0}\left(1-\alpha^2\right)\sqrt{1-\beta^2}, \\
\mathcal{P}_x &= \frac{\Delta_{\mathrm{SAS}}}{\Delta_0}\alpha^2\sqrt{1-\beta^2}, \\
\mathcal{P}_z &= \frac{\Delta_{\mathrm{SAS}}}{\Delta_0}\alpha^2\beta.
\end{aligned}
\tag{4.1}
$$

Recall that $\mathcal{S}_x = \mathcal{S}_y = 0$ and $\mathcal{P}_y = 0$. Using (3.26) in (3.25), we perform all the necessary substitutions and obtain

$$
\begin{aligned}
\mathcal{R}_{xx} + i\mathcal{R}_{yx} &= -\frac{\Delta_{\mathrm{SAS}}}{\Delta_0}\alpha\sqrt{1-\alpha^2}\beta e^{i\omega}, \\
\mathcal{R}_{yy} + i\mathcal{R}_{xy} &= +\frac{\Delta_{\mathrm{Z}}}{\Delta_0}\alpha\sqrt{1-\alpha^2}\sqrt{1-\beta^2}e^{i\omega}, \\
\mathcal{R}_{xz} + i\mathcal{R}_{yz} &= +\frac{\Delta_{\mathrm{SAS}}}{\Delta_0}\alpha\sqrt{1-\alpha^2}\sqrt{1-\beta^2}e^{i\omega}, \quad
\end{aligned}
\tag{4.2}
$$

while the rest components vanish, $\mathcal{R}_{za} = 0$. We have expressed all the isospin components $\mathcal{S}_a$, $\mathcal{P}_a$ and $\mathcal{R}_{ab}$ in terms of three variables α, β and ω.

Using $2\mathcal{S}_a^{\mathrm{f}} = \mathcal{S}_a + \mathcal{R}_{az}$ and $2\mathcal{S}_a^{\mathrm{b}} = \mathcal{S}_a - \mathcal{R}_{az}$ we find

$$
\begin{aligned}
\mathcal{S}_x^{\mathrm{f}} = -\mathcal{S}_x^{\mathrm{b}} &= \frac{1}{2}\frac{\Delta_{\mathrm{SAS}}}{\Delta_0}\alpha\sqrt{1-\alpha^2}\sqrt{1-\beta^2}\cos\omega, \\
\mathcal{S}_y^{\mathrm{f}} = -\mathcal{S}_y^{\mathrm{b}} &= \frac{1}{2}\frac{\Delta_{\mathrm{SAS}}}{\Delta_0}\alpha\sqrt{1-\alpha^2}\sqrt{1-\beta^2}\sin\omega.
\end{aligned}
\tag{4.3}
$$

We see that ω describes the orientation of $\mathcal{S}_a^{\mathrm{f}}$ and $\mathcal{S}_a^{\mathrm{b}}$ in the xy-plane. It is the zero-energy mode associated with the rotational invariance in the xy-plane.

Employing the formulae derived in Appendix C, the matrix g can be reconstructed from (4.1) and (4.2). For the sake of simplicity we take $\omega = \frac{\pi}{4}$ and come to

$$
g = \gamma_\uparrow^{\mathrm{s}}g_\uparrow^{\mathrm{s}} + \gamma_0^{\mathrm{s}}g_0^{\mathrm{s}} + \gamma_\downarrow^{\mathrm{s}}g_\downarrow^{\mathrm{s}} + \gamma_{\mathrm{f}}^{\mathrm{p}}g_{\mathrm{f}}^{\mathrm{p}} + \gamma_0^{\mathrm{p}}g_0^{\mathrm{p}} + \gamma_{\mathrm{b}}^{\mathrm{p}}g_{\mathrm{b}}^{\mathrm{p}}, \tag{4.4}
$$

where

$$
\begin{aligned}
g_\uparrow^{\mathrm{s}} &= \frac{i}{2}\left(1+\tau_z^{\mathrm{spin}}\right)\tau_y^{\mathrm{ppin}}, & g_{\mathrm{f}}^{\mathrm{p}} &= \frac{i}{2}\tau_y^{\mathrm{spin}}\left(1+\tau_z^{\mathrm{ppin}}\right), \\
g_0^{\mathrm{s}} &= \frac{i}{2}\sqrt{2}\tau_x^{\mathrm{spin}}\tau_y^{\mathrm{ppin}}, & g_0^{\mathrm{p}} &= \frac{i}{2}\sqrt{2}\tau_y^{\mathrm{spin}}\tau_x^{\mathrm{ppin}}, \\
g_\downarrow^{\mathrm{s}} &= \frac{i}{2}\left(1-\tau_z^{\mathrm{spin}}\right)\tau_y^{\mathrm{ppin}}, & g_{\mathrm{b}}^{\mathrm{p}} &= \frac{i}{2}\tau_y^{\mathrm{spin}}\left(1-\tau_z^{\mathrm{ppin}}\right).
\end{aligned}
\tag{4.5}
$$

and

$$
\begin{aligned}
\gamma_\uparrow^{\mathrm{s}} &= \frac{1+i}{2\sqrt{2}}\sqrt{1-\alpha^2}\left(1+\frac{\Delta_{\mathrm{Z}}}{\Delta_0}\sqrt{1-\beta^2}\right), \\
\gamma_0^{\mathrm{s}} &= 0, \\
\gamma_\downarrow^{\mathrm{s}} &= \frac{1-i}{2\sqrt{2}}\sqrt{1-\alpha^2}\left(1-\frac{\Delta_{\mathrm{Z}}}{\Delta_0}\sqrt{1-\beta^2}\right), \\
\gamma_{\mathrm{f}}^{\mathrm{p}} &= -\frac{i\alpha}{2}\left(1+\frac{\Delta_{\mathrm{SAS}}}{\Delta_0}\beta\right), \\
\gamma_0^{\mathrm{p}} &= -\frac{i\alpha}{\sqrt{2}}\frac{\Delta_{\mathrm{SAS}}}{\Delta_0}\sqrt{1-\beta^2}, \\
\gamma_{\mathrm{b}}^{\mathrm{p}} &= -\frac{i\alpha}{2}\left(1-\frac{\Delta_{\mathrm{SAS}}}{\Delta_0}\beta\right).
\end{aligned}
\tag{4.6}
$$

Equivalently, the ground state is expressed as

$$
\begin{aligned}
|\mathrm{g}(n)\rangle =\; &\gamma_\uparrow^{\mathrm{s}}|\mathcal{S}_\uparrow(n)\rangle + \gamma_0^{\mathrm{s}}|\mathcal{S}_0(n)\rangle + \gamma_\downarrow^{\mathrm{s}}|\mathcal{S}_\downarrow(n)\rangle \\
&+ \gamma_{\mathrm{f}}^{\mathrm{p}}|\mathcal{P}_{\mathrm{f}}(n)\rangle + \gamma_0^{\mathrm{p}}|\mathcal{P}_0(n)\rangle + \gamma_{\mathrm{b}}^{\mathrm{p}}|\mathcal{P}_{\mathrm{b}}(n)\rangle, \quad
\end{aligned}
\tag{4.7}
$$

where

$$
\begin{aligned}
|\mathcal{S}_\uparrow(n)\rangle &= c_{\mathrm{f}\uparrow}^\dagger(n)c_{\mathrm{b}\uparrow}^\dagger(n)|0\rangle, \\
|\mathcal{S}_0(n)\rangle &= \frac{c_{\mathrm{f}\uparrow}^\dagger(n)c_{\mathrm{b}\downarrow}^\dagger(n) + c_{\mathrm{f}\downarrow}^\dagger(n)c_{\mathrm{b}\uparrow}^\dagger(n)}{\sqrt{2}}|0\rangle, \\
|\mathcal{S}_\downarrow(n)\rangle &= c_{\mathrm{f}\downarrow}^\dagger(n)c_{\mathrm{b}\downarrow}^\dagger(n)|0\rangle, \\
|\mathcal{P}_{\mathrm{f}}(n)\rangle &= c_{\mathrm{f}\uparrow}^\dagger(n)c_{\mathrm{f}\downarrow}^\dagger(n)|0\rangle, \\
|\mathcal{P}_0(n)\rangle &= \frac{c_{\mathrm{f}\uparrow}^\dagger(n)c_{\mathrm{b}\downarrow}^\dagger(n) - c_{\mathrm{f}\downarrow}^\dagger c_{\mathrm{b}\uparrow}^\dagger(n)}{\sqrt{2}}|0\rangle, \\
|\mathcal{P}_{\mathrm{b}}(n)\rangle &= c_{\mathrm{b}\uparrow}^\dagger(n)c_{\mathrm{b}\downarrow}^\dagger(n)|0\rangle.
\end{aligned}
\tag{4.8}
$$

This reveals the microscopic structure of the ground state.

All quantities are parametrized by α and β. When we solve (3.36a) and (3.36b) for them, we find $\alpha < 0$ for $\Delta_{\mathrm{bias}} < \Delta_{\mathrm{bias}}^{\mathrm{sc}}$, and $\alpha > 1$ for $\Delta_{\mathrm{bias}} > \Delta_{\mathrm{bias}}^{\mathrm{pc}}$ with certain values of $\Delta_{\mathrm{bias}}^{\mathrm{sc}}$ and $\Delta_{\mathrm{bias}}^{\mathrm{pc}}$: see (5.7). Accordingly the ground-state energy (3.35) is minimized by $\alpha = 0$ for $\Delta_{\mathrm{bias}} < \Delta_{\mathrm{bias}}^{\mathrm{sc}}$, and $\alpha = 1$ for $\Delta_{\mathrm{bias}} > \Delta_{\mathrm{bias}}^{\mathrm{pc}}$. Then, the spin component $\mathcal{S}_z$ and the density imbalance $\mathcal{P}_z$ are calculated from (4.1). In FIG.1 we illustrate $\mathcal{S}_z$ and $\sigma_0 \equiv \mathcal{P}_z$ together with α as functions of Δ_{bias} for typical sample parameters; $d = 23$nm, $\Delta_{\mathrm{SAS}} = 6.7$K and $\rho_0 = n \times 10^{11}/\mathrm{cm}^2$ with $n = 1.4$ and $= 0.9$.

First, when $\alpha = 0$, it follows that $\mathcal{S}_z = 1$ and $\mathcal{P}_z = 0$ since $\Delta_0 = \Delta_{\mathrm{Z}}\sqrt{1-\beta^2}$. Note that β disappears from all formulas in (4.6). The spin phase is characterized by the fact that the isospin is fully polarized into the spin direction with $\mathcal{S}_z = 1$ and all others being zero. The spins in both layers point to the positive z-axis due to the Zeeman effect. Substituting $\alpha = 0$ and $\Delta_0 \equiv \Delta_{\mathrm{Z}}\sqrt{1-\beta^2}$ into (4.6) we find the ground state to be

$$
|\mathrm{g}_{\mathrm{spin}}\rangle = \prod_n c_{\mathrm{f}\uparrow}^\dagger(n)c_{\mathrm{b}\uparrow}^\dagger(n)|0\rangle. \tag{4.9}
$$

It is interesting to notice that, even if the bias voltage is applied, no charge transfer occurs between the two layers ($\sigma_0 = 0$) as far as $\Delta_{\text{bias}} < \Delta_{\text{bias}}^{\text{sc}}$, where the system is in the spin phase [FIG.1].

Second, when $\alpha = 1$, it follows that $\mathcal{S}_z = 0$ and $\mathcal{P}_z \neq 0$ (actually $\mathcal{P}_x^2 + \mathcal{P}_z^2 = 1$). The ppin phase is characterized by the fact that the isospin is fully polarized into the pseudospin direction with

$$\mathcal{P}_x = \sqrt{1 - \beta^2}, \qquad \mathcal{P}_z = \beta, \qquad (4.10)$$

and all others being zero. Because $\mathcal{P}_z$ represents the density difference between the two layers, β is identified with the imbalance parameter σ_0. Substituting $\alpha = 1$ into (4.6) we obtain the ground state as

$$|g_{\text{ppin}}\rangle = \prod_n \left\{ \frac{1}{2} \left(\sqrt{1 + \sigma_0} c_{\text{f}\uparrow}^\dagger(n) + \sqrt{1 - \sigma_0} c_{\text{b}\uparrow}^\dagger(n) \right) \right.$$
$$\left. \times \left(\sqrt{1 + \sigma_0} c_{\text{f}\downarrow}^\dagger(n) + \sqrt{1 - \sigma_0} c_{\text{b}\downarrow}^\dagger(n) \right) \right\} |0\rangle.$$
$$(4.11)$$

It is found that all electrons are in the front layer when $\sigma_0 = 1$, and in the back layer when $\sigma_0 = -1$.

For intermediate values of α ($0 < \alpha < 1$) none of the spin and pseudospin vanish, where we may control the density imbalance by applying a bias voltage as in the ppin phase. The ground state $|g_{\text{cant}}\rangle$ is given by (4.7) with (4.6). All states except $|\mathcal{S}_0(n)\rangle$ contribute to form the ground state. This is so even in the balanced configuration ($\beta = 0$). It follows from (4.1) and (4.3) that, as the system goes away from the spin phase, the spin begin to cant and make antiferromagnetic correlations between the two layers. Hence, it is called the canted antiferromagnetic phase[4].

We conclude that there are three phases in general; the spin phase, the canted phase and the ppin phase. They are as characterized by

spin	canted	ppin
$\boldsymbol{S}^2 = 1$	$\boldsymbol{S}^2 \neq 0$	$\boldsymbol{S}^2 = 0$
$\boldsymbol{\mathcal{P}}^2 = 0$	$\boldsymbol{\mathcal{P}}^2 \neq 0$	$\boldsymbol{\mathcal{P}}^2 = 1$

$$(4.12)$$

The order parameters are $\boldsymbol{S}^2$ and $\boldsymbol{\mathcal{P}}^2$.

Let us study the system with no bias voltage in more detail. The spin and pseudospin are

$$\mathcal{S}_z = \frac{\Delta_Z}{\sqrt{\Delta_{\text{SAS}}^2 \alpha^2 + \Delta_Z^2 (1 - \alpha^2)}} (1 - \alpha^2),$$
$$\mathcal{P}_x = \frac{\Delta_{\text{SAS}}}{\sqrt{\Delta_{\text{SAS}}^2 \alpha^2 + \Delta_Z^2 (1 - \alpha^2)}} \alpha^2, \qquad (4.13)$$

where α^2 is easily obtained from (3.36a) with $\beta = 0$,

$$\alpha^2 = \frac{\Delta_{\text{SAS}}^2 - \Delta_Z^2}{4(2\varepsilon_X^-)^2} - \frac{\Delta_Z^2}{\Delta_{\text{SAS}}^2 - \Delta_Z^2}. \qquad (4.14)$$
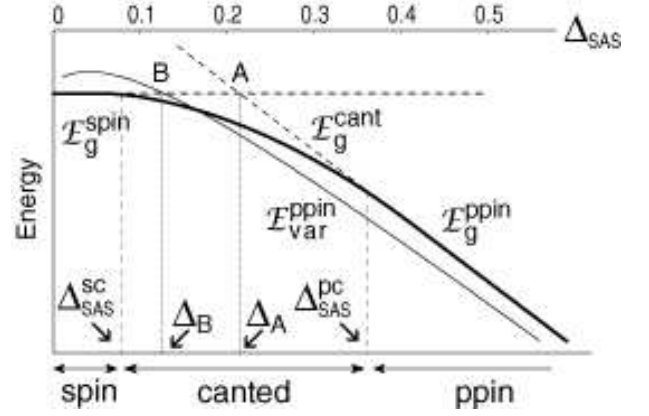

FIG. 2: The ground-state energies $\mathcal{E}_g^{\text{spin}}$, $\mathcal{E}_g^{\text{ppin}}$ and $\mathcal{E}_g^{\text{cant}}$ are given in the spin, ppin and canted phases in the balanced configuration by taking $d = 0.56\ell_B$. The horizontal axis is the tunneling gap Δ_{SAS} in the Coulomb unit $E_C^0 = e^2/(4\pi\varepsilon\ell_B)$. A phase transition occurs along the heavy curve continuously from the spin phase to the canted phase, and then to the ppin phase, as Δ_{SAS} increases. The phase transition points $\Delta_{\text{SAS}}^{\text{sc}}$ and $\Delta_{\text{SAS}}^{\text{pc}}$ are given by (4.17) and (4.18) in the first order of perturbation. The energy $\mathcal{E}_g^{\text{spin}}$ is not modified but $\mathcal{E}_g^{\text{ppin}}$ is modified into $\mathcal{E}_{\text{var}}^{\text{ppin}}$ by higher order quantum corrections. The point A stands for the would-be crossing of the spin and ppin energy levels in the first order of perturbation, with Δ_A given by (4.16). The point B stands for the one when higher order quantum corrections are taken into account, with Δ_B given by (6.13), suggesting that the canted phase is considerably shrunk.

The ground-state energy in each phase is given by

$$\mathcal{E}_g^{\text{spin}} = -2\varepsilon_X^+ - 2\varepsilon_X^- - \Delta_Z,$$
$$\mathcal{E}_g^{\text{cant}} = -2\varepsilon_X^+ - \frac{\Delta_{\text{SAS}}^2}{8\varepsilon_X^-} + \frac{\Delta_Z^2}{8\varepsilon_X^-} - \frac{2\varepsilon_X^- \Delta_{\text{SAS}}^2}{\Delta_{\text{SAS}}^2 - \Delta_Z^2},$$
$$\mathcal{E}_g^{\text{ppin}} = -2\varepsilon_X^+ - \Delta_{\text{SAS}}. \qquad (4.15)$$

We have depicted them as a function of Δ_{SAS} in FIG.2.

If the canted phase were ignored, the two levels $\mathcal{E}_g^{\text{spin}}$ and $\mathcal{E}_g^{\text{ppin}}$ would cross at

$$\Delta_{\text{SAS}}^{\text{sp}} = \Delta_Z + 2\varepsilon_X^-, \qquad (4.16)$$

and a transition would occur suddenly from the spin phase ($\boldsymbol{S}^2 = 1$, $\boldsymbol{\mathcal{P}}^2 = 0$) to the ppin phase ($\boldsymbol{S}^2 = 0$, $\boldsymbol{\mathcal{P}}^2 = 1$). Actually, a mixing of states occurs and lowers the ground state energy. As a result the level crossing turns into an level anticrossing [FIG.2], and the canted state emerges between the spin and ppin phases. As Δ_{SAS} increases, the phase transition occurs continuously from the spin phase to the canted phase, and then to the ppin phase. The phase transition points are

$$\Delta_{\text{SAS}}^{\text{sc}} = \sqrt{\Delta_Z^2 + 4\varepsilon_X^- \Delta_Z} \qquad (4.17)$$

from $\mathcal{E}_g^{\text{spin}} = \mathcal{E}_g^{\text{cant}}$, and

$$\Delta_{\text{SAS}}^{\text{pc}} = 2\varepsilon_X^- + \sqrt{\Delta_Z^2 + (2\varepsilon_X^-)^2} \qquad (4.18)$$

from $\mathcal{E}_g^{\mathrm{ppin}} = \mathcal{E}_g^{\mathrm{cant}}$. These two formulas agree with the variational result due to MacDonald et al.[13], where the variational state has been chosen from a subset of the full set (3.2) satisfying (3.5).

V. PHASE DIAGRAMS

The phase diagram can be studied based on analytic formulas given in the previous section. We first present the phase diagram in the Δ_{SAS}-Δ_{Z} plane for typical values of Δ_{bias} to compare our result with the standard ones[8,13]. We search for the boundaries separating the canted phase from the spin and ppin phases in the system. These are extracted from (3.36a) and (3.36b). The merit of our formalism is that analytic expressions are available to determine the phase boundaries even for imbalanced configurations.

Along the spin-canted boundary we have $\alpha = 0$. Substituting this value into (3.36b) we get

$$\frac{\beta}{\sqrt{1-\beta^2}} = \frac{\Delta_{\mathrm{bias}}}{\Delta_{\mathrm{SAS}}} \frac{\Delta_{\mathrm{Z}}}{\Delta_{\mathrm{Z}} + 4\varepsilon_{\mathrm{X}}^-}. \tag{5.1}$$

We solve this for β and substitute it into (3.36a) to get

$$\Delta_{\mathrm{SAS}}^2 = \Delta_{\mathrm{Z}}^2 + 4\varepsilon_{\mathrm{X}}^-\Delta_{\mathrm{Z}} - \frac{\Delta_{\mathrm{Z}}\Delta_{\mathrm{bias}}^2}{\Delta_{\mathrm{Z}} + 4\varepsilon_{\mathrm{X}}^-}. \tag{5.2}$$

This determines the spin-canted boundary.

Along the ppin-canted boundary we have $\alpha = 1$. Substituting this value into (3.36a) and (3.36b) we get

$$\Delta_{\mathrm{SAS}} = \sqrt{1-\beta^2}\left[\frac{\Delta_{\mathrm{bias}}}{\beta} - 2\varepsilon_{\mathrm{cap}}\right] \tag{5.3}$$

and

$$\Delta_{\mathrm{Z}}^2 = \left(\frac{\Delta_{\mathrm{bias}}}{\beta} - 2\varepsilon_{\mathrm{cap}}\right)\left(\frac{\Delta_{\mathrm{bias}}}{\beta} - 8\varepsilon_{\mathrm{D}}^- + 4\beta^2\varepsilon_{\mathrm{X}}^-\right) \tag{5.4}$$

after some manipulation. These two equations give a parametric representation of the ppin-canted boundary in terms of β.

In drawing the phase diagram in the Δ_{SAS}-Δ_{Z} plane we need to fix the layer separation d. Following the standard literature[8,13], we have examined the case $d = \ell_B$ and presented the phase diagram in FIG.3. Our results agree qualitatively with results obtained numerically by Brey et al.[8] and MacDonald et al.[13] for imbalanced configurations.

Our analytic formulas reveal some new features not reported in literature. We have found some peculiar behaviors for the ppin-canted boundary as in FIG.4, which occurs for $2\varepsilon_{\mathrm{D}}^- < 3\varepsilon_{\mathrm{X}}^-$, or $d \lesssim 0.75\ell_B$. When the bias voltage is increased, a small ppin region appears in the vicinity of the origin at

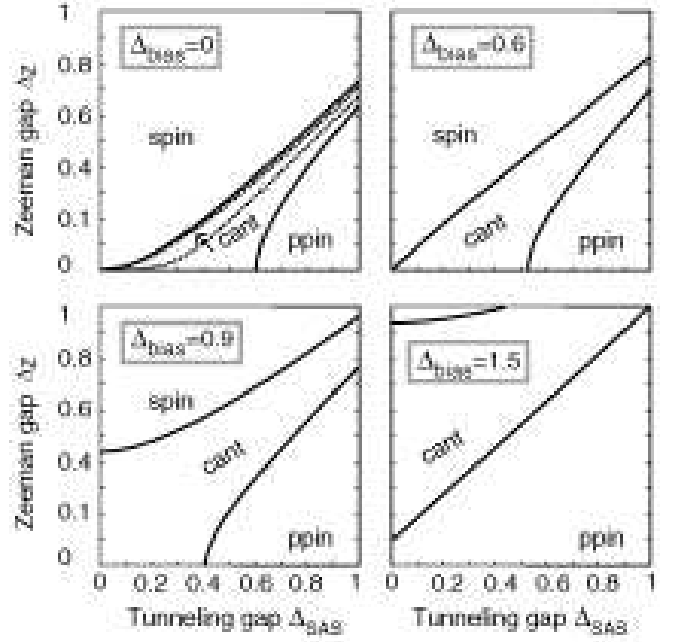$$\Delta_{\mathrm{B}}^{(1)} = 2\varepsilon_{\mathrm{cap}}. \tag{5.5}$$

FIG. 3: The phase diagram is given in the Δ_{SAS}-Δ_{Z} plane by changing the bias energy Δ_{bias}. Here we have set $d = \ell_B$, and taken the Coulomb energy unit E_{C}^0 for the tunneling gap (horizontal axis) and the Zeeman gap (vertical axis). It is observed that both the canted and ppin phases are stabilized even for $\Delta_{\mathrm{SAS}} = 0$ by applying the bias voltage. The dotted curves in the top left panel represent the exact diagonalization result due to Schliemann et al.[9] for the 12 electron system. It is observed that the ppin-canted phase boundary is modified considerably by higher oder quantum corrections.

This region is isolated from the basic ppin region by the canted phase. By increasing Δ_{bias}, the isolated and basic ppin regions come closer, and they merge at

$$\Delta_{\mathrm{B}}^{(2)} = 8\left[\frac{2\varepsilon_{\mathrm{D}}^-}{3\varepsilon_{\mathrm{X}}^-}\right]^{\frac{3}{2}}\varepsilon_{\mathrm{X}}^-. \tag{5.6}$$

Then the isolated region disappears.

These phase diagrams are, however, not so useful to analyze experimental data, since we need many samples with different d to realize, e.g., $d = \ell_B$, but this is impossible. It is more interesting to see experimentally[7] how the phase transition occurs by controlling the total density ρ_0 and also the imbalance parameter σ_0 in a single sample with fixed values of d and Δ_{SAS}. Here we wish to describe new aspects of the phase diagram from this point of view.

We start with the spin phase in the balanced configuration with $\Delta_{\mathrm{bias}} = 0$. (The spin phase realizes provided the electron density is more than a certain critical value.) When the bias voltage is applied ($\Delta_{\mathrm{bias}} \neq 0$) the parameter β becomes nonzero according to (5.1). However, no charge imbalance is induced between the two layers ($\sigma_0 = 0$) as far as $\alpha = 0$. A charge imbalance occurs only above a certain critical value $\Delta_{\mathrm{bias}}^{\mathrm{sc}}$ of the bias voltage as
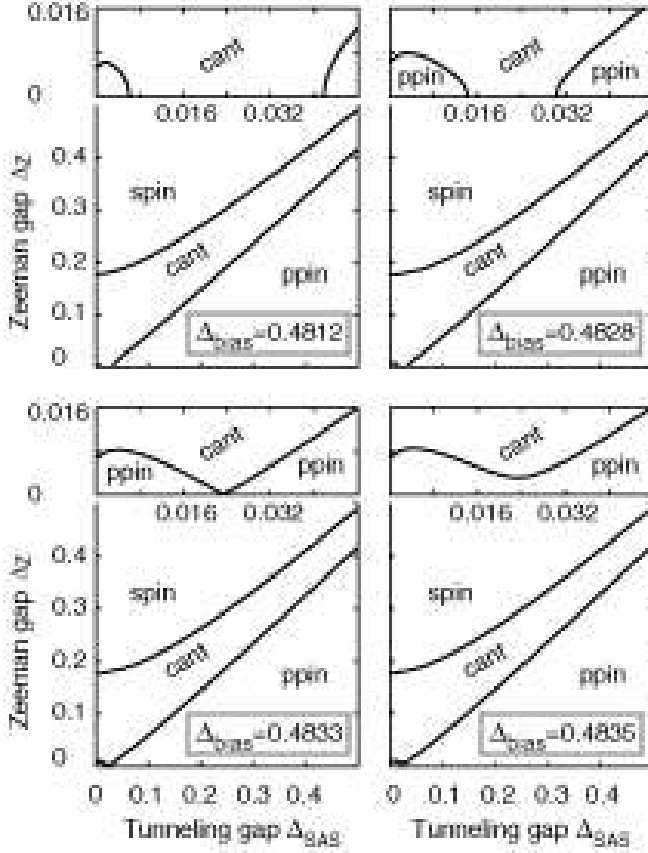
FIG. 4: The phase diagram is given in the Δ_{SAS}-Δ_{Z} plane by changing the bias energy Δ_{bias}. Here we have set $d = 0.4\ell_B$, and taken the Coulomb energy unit E_{C}^0 for the tunneling gap (horizontal axis) and the Zeeman gap (vertical axis). A small ppin region appears in the vicinity of the origin for $d \lesssim 0.75\ell_B$. This region is isolated from the basic ppin region by the canted phase. This is shown in the top left panel. The upper part of each panel is the enlarged image of the vicinity of origin where the isolated ppin region appears.

in FIG.1, which is given by solving (5.2) as

$$(\Delta_{\text{bias}}^{\text{sc}})^2 = (\Delta_{\text{Z}} + 4\varepsilon_{\text{X}}^-)^2 - \left(1 + 4\frac{\varepsilon_{\text{X}}^-}{\Delta_{\text{Z}}}\right)\Delta_{\text{SAS}}^2. \quad (5.7)$$

This gives the spin-canted phase boundary in the Δ_{bias}-ρ_0 plane [FIG.5]. For $\Delta_{\text{bias}} > \Delta_{\text{bias}}^{\text{sc}}$ the system is driven into the canted phase with $\alpha \neq 0$. As the bias voltage increases above a second critical value $\Delta_{\text{bias}}^{\text{pc}}$, the system turns into the ppin phase with $\alpha = 1$ as in FIG.1. The critical value $\Delta_{\text{bias}}^{\text{pc}}$ is obtained by eliminating β in (5.3) and (5.4). This gives the ppin-canted phase boundary in the Δ_{bias}-ρ_0 plane [FIG.5]. We remark that, as the electron density decreases, the critical point $\Delta_{\text{bias}}^{\text{sc}}$ decreases and eventually becomes zero so that the spin phase disappears at all: The critical density is $\rho_0 = 1.19 \times 10^{11}/\text{cm}^{-2}$ in the case of FIG.5.

To compare the experimental data[7,14] it is more convenient to present the phase diagram in the σ_0-ρ_0 plane [FIG.6], which is constructed by using the relation be-
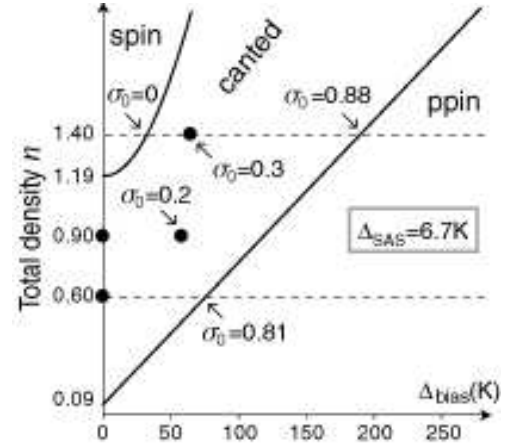

FIG. 5: The phase diagram is given in the Δ_{bias}-ρ_0 plane for the sample with $d = 23$nm, where $\rho_0 = n \times 10^{11}/\text{cm}^{-2}$. The two curves stand for the spin-canted phase boundary and the ppin-canted phase boundary in the first order of perturbation. The four large points are experimental data indicating phase transition points taken from Sawada et al.[7].
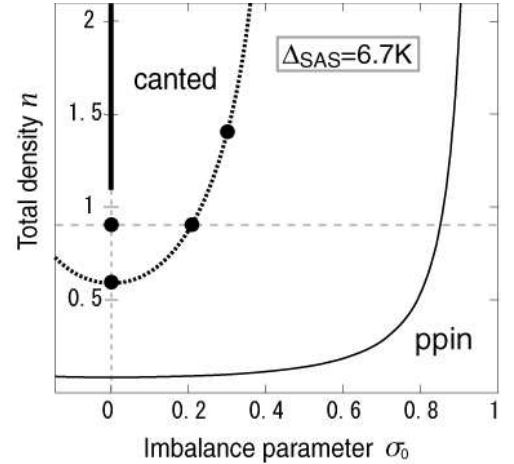

FIG. 6: The phase diagram is given in the σ_0-ρ_0 plane, where the sample parameters are the same as in FIG. 5. The spin phase is realized only in the balance configuration ($\sigma_0 = 0$) along the heavy line. The solid curve represents the ppin-canted phase boundary in the first order of perturbation. The four large points are experimental data indicating phase transition points taken from Sawada et al.[7]. The dotted curve is a speculated ppin-canted phase boudary. The dotted horizontal line at $n = 0.9$ corresponds to the plateau-width curve indexed by $n = 0.9$ in FIG.8(b).

tween the bias voltage and the imbalance parameter implied by (5.3) and (5.4).

It is also useful to study the phase diagram in the ρ_0-Δ_{SAS} plane, since it is not difficult to prepare samples with different Δ_{SAS} with all other parameters unchanged [FIG.7]. This is constructed from (4.17) and (4.18).
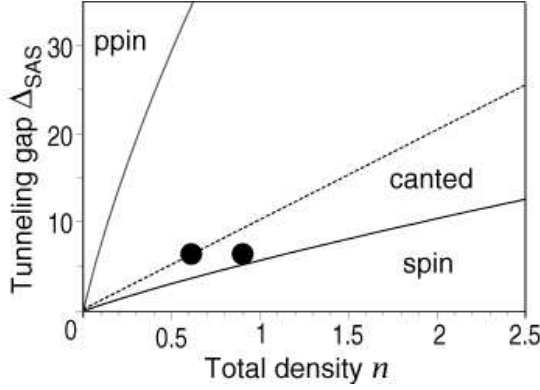
FIG. 7: The phase diagram is given in the ρ_0-Δ_{SAS} plane at the balance point, where the sample parameters are the same as in FIG. 5. The horizontal axis denotes the total density $\rho_0 = n \times 10^{11}/\mathrm{cm}^2$, while the vertical axis denotes the tunneling gap Δ_{SAS} in Kelvin. The dotted curve is a speculated ppin-canted phase boundary. The two large points are experimental data indicating phase transition points taken from Sawada et al.[7].

VI. HIGHER ORDER CORRECTIONS

We have explored the ground-state structure in the first order of perturbation theory. Our Hamiltonian consists of the SU(4)-invariant term H_C^+ and the SU(4)-noninvariant term $H_{\mathrm{non}} = H_C^- + H_{\mathrm{ZpZ}}$. We are interested in the regime where $H_C^+ \gg H_{\mathrm{non}}$. Hence we have diagonalized H_C^+ as in (3.4) and treat H_{non} perturbatively. The eigenstates are degenerate with respect to H_C^+, consisting of 6 states at each Landau site. The degeneracy is removed by the SU(4)-noninvariant terms H_{non}. We may construct 6 states $|g_i\rangle$ satisfying

$$\langle g_j | g_i \rangle = \delta_{ij}, \qquad \langle g_j | H | g_i \rangle = E_i \delta_{ij} \qquad (6.1)$$

as follows. First we determine $|g_0\rangle$ by minimizing $\langle g | H | g \rangle$ with the use of a general state (4.7). We then construct a Fock space made of 5 states that are orthogonal to $|g_0\rangle$. Within this space we can minimize $\langle g | H | g \rangle$, which determines the lowest energy state $|g_1\rangle$. In this way we may construct 6 states $|g_0\rangle, \cdots, |g_5\rangle$ with $E_0 \le E_1 \le \cdots \le E_5$, which satisfy (6.1). The full Hamiltonian is diagonalized within the first order perturbation theory.

We have constructed the phase boundaries between the spin phase, the canted phase and the ppin phase. Here we recall the exact-diagonalization result[9] of a few-electron system showing that the boundary between the spin and canted phases is practically unmodified but the boundary between the canted and ppin phases is considerably modified from the mean-field result [FIG.3]. In order to explain this we discuss effects due to higher order perturbations.

We start with the spin phase. It is important that the fully spin polarized state (4.9) is an exact eigenstate of the total Hamiltonian H. This follows from

$$P_z(i,j)|g_{\mathrm{spin}}\rangle = P_x(i,j)|g_{\mathrm{spin}}\rangle = 0 \qquad (6.2)$$

and

$$S_z(i,i)|g_{\mathrm{spin}}\rangle = 1. \qquad (6.3)$$

We obtain $H|g_{\mathrm{spin}}\rangle = \mathcal{E}_g^{\mathrm{spin}}|g_{\mathrm{spin}}\rangle$ with

$$\mathcal{E}_g^{\mathrm{spin}} = -\left(2\varepsilon_X^+ + 2\varepsilon_X^- + \Delta_Z\right). \qquad (6.4)$$

The eigenvalue agrees with the mean-field value in (4.15). Hence the mean-field equations (3.36a) $\sim$ (3.36c) are exact ones in the spin phase, implying that the spin-canted phase boundary is not affected by higher order perturbations.

We proceed to discuss the ppin phase. For simplicity we consider the balanced point, where

$$S_z(i,i)|g_{\mathrm{ppin}}\rangle = 1, \quad P_z(i,i)|g_{\mathrm{ppin}}\rangle = 0. \qquad (6.5)$$

However, since

$$P_z(i,j)|g_{\mathrm{ppin}}\rangle \ne 0 \quad \text{for} \quad i \ne j, \qquad (6.6)$$

though $\langle g_{\mathrm{ppin}}|P_z(i,j)|g_{\mathrm{ppin}}\rangle = 0$, the state $|g_{\mathrm{ppin}}\rangle$ is not an eigenstate of the capacitance term H_C^-. Hence the fully pseudospin polarized state (4.11) is not an eigenstate of the total Hamiltonian H even in the absence of the tunneling interaction ($\Delta_{\mathrm{SAS}} = 0$).

It is practically impossible to carry out the second order perturbation since almost no eigenstates of the unperturbed Hamiltonian H_C^+ are known. We make a variational analysis. We decompose the total Hamiltonian H into two pieces, H_0 and H_1, where H_0 is the maximal part of H one of whose eigenstates is $|g_{\mathrm{ppin}}\rangle$. We do not give their explicit forms here since they are very complicated. We obtain

$$H_0|g_{\mathrm{ppin}}\rangle = \mathcal{E}_g^{\mathrm{ppin}}|g_{\mathrm{ppin}}\rangle \qquad (6.7)$$

with

$$\mathcal{E}_g^{\mathrm{ppin}} = -2\varepsilon_X^+ - \varepsilon_{\mathrm{cap}}\sigma_0^2 - \frac{\Delta_{\mathrm{SAS}}}{\sqrt{1-\sigma_0^2}}. \qquad (6.8)$$

This agrees with the first-order perturbation result (4.15) at $\sigma_0 = 0$. Hence the variational analysis surely presents a higher order correction. According to the standard procedure, we minimize the total energy with the variational state

$$|g_{\mathrm{ppin}}^{\mathrm{var}}\rangle = (1 + \lambda H_1)|g_{\mathrm{ppin}}\rangle, \qquad (6.9)$$

where λ is the variational parameter. Then the energy reads

$$\mathcal{E}_{\mathrm{var}}^{\mathrm{ppin}} = \mathcal{E}_g^{\mathrm{ppin}} + \frac{|\langle g_{\mathrm{ppin}}|H_1^2|g_{\mathrm{ppin}}\rangle|^2}{\mathcal{E}_g^{\mathrm{ppin}}\langle g_{\mathrm{ppin}}|H_1^2|g_{\mathrm{ppin}}\rangle - \langle g_{\mathrm{ppin}}|H_1 H_0 H_1|g_{\mathrm{ppin}}\rangle}. \qquad (6.10)$$

The calculation is straightforward though quite tedious. To perform various integrals explicitly we approximate (2.5) as

$$V^+(\boldsymbol{q}) = \frac{1}{|\boldsymbol{q}|}\exp\left(-\frac{1}{2}|\boldsymbol{q}|^2\right)E_C^0,$$

$$V^-(\boldsymbol{q}) = \frac{d}{2}\exp\left(-\frac{1}{2}|\boldsymbol{q}|^2\right)E_C^0 \qquad (6.11)$$

with $E_C^0 = e^2/(4\pi\varepsilon\ell_B)$, which is valid for $d/\ell_B \ll 1$. The result is given by

$$\mathcal{E}_{\text{var}}^{\text{ppin}} = \mathcal{E}_{\text{g}}^{\text{ppin}} - \frac{d^2}{16\ell_B^2} \frac{(1-\sigma_0^2)^2 E_C^0}{\sqrt{\pi}\left(\frac{1}{2} + \frac{1}{\sqrt{2}} - \frac{2}{\sqrt{3}}\right) + \frac{\Delta_{\text{SAS}}/E_C^0}{\sqrt{1-\sigma_0^2}}}.$$
(6.12)

The correction is larger for larger layer separation d, and it is largest at the balanced point ($\sigma_0 = 0$).

It is not easy to derive higher order corrections for the canted phase, since $|g_{\text{cant}}\rangle$ is not an eigenstate of any simple Hamiltonian and furthermore it is a complicated state involving 5 states as in (4.7). Though we are unable to determine the improved ppin-canted phase boundary, we may make some arguments how it is modified. For simplicity we study the balanced point. We have shown that the would-be phase transition point is $\Delta_{\text{SAS}}^{\text{sp}}$ given by (4.16) in the ignorance of the canted phase. We examine how this point is modified by equating (6.4) and (6.12). Namely, from $\mathcal{E}_{\text{g}}^{\text{spin}} = \mathcal{E}_{\text{var}}^{\text{ppin}}$ we find

$$\frac{\Delta_{\text{SAS}}^{\text{var}}}{E_C^0} = \frac{1}{2}\left(\frac{\Delta_{\text{SAS}}^{\text{sp}}}{E_C^0} - 0.1 + \sqrt{\left(\frac{\Delta_{\text{SAS}}^{\text{sp}}}{E_C^0} + 0.1\right)^2 - \frac{d^2}{4\ell_B^2}}\right).$$
(6.13)

It is observed that this is much smaller than the first order perturbation result [FIG.2]. Since the spin-canted boundary (4.17) is not modified we expect that the canted phase is shrunk considerably. These features are precisely what are found in the exact diagonalization of a few electron system[9] [FIG.3].

VII. EXPERIMENTAL STATUS

Based on our theoretical results we wish to interpret the experimental data due to Sawada et el.[7,14] yielding an unambiguous evidence for phase transitions. They have presented the activation-energy data for ρ_0 [FIG.8(a)] and the plateau-width data for σ_0 [FIG.8(b)]. In this section we set $\rho_0 = n \times 10^{11}/\text{cm}^2$, and use n to represent the total density.

We see a phase transition point $(\sigma_0, n) = (0, 0.9)$ from the activation-energy data [FIG.8(a)], for which $d/\ell_B = 1.23$ in the sample with $d = 23\text{nm}$. We give the phase diagram in Δ_{SAS}-Δ_{Z} plane, upon which we plot the data point [FIG.9]. On one hand, the point is almost on the spin-canted boundary. Furthermore, though the spin-canted boundary is exact, it is obtained in the ideal two-dimensional system and it will be modified in actual samples with finite quantum wells. Then it is reasonable that the point is slightly off the theoretical estimation. On the other hand, as we have argued, the ppin-canted phase boundary is considerably modified so that the canted phase occupies a tiny domain in the phase diagram [FIG.2 and FIG.3]. We cannot compare the exact diagonalization result[9] with the data directly since it is available only at $V_{\text{bias}} = 0$ and $d/\ell_B = 1$. Since the
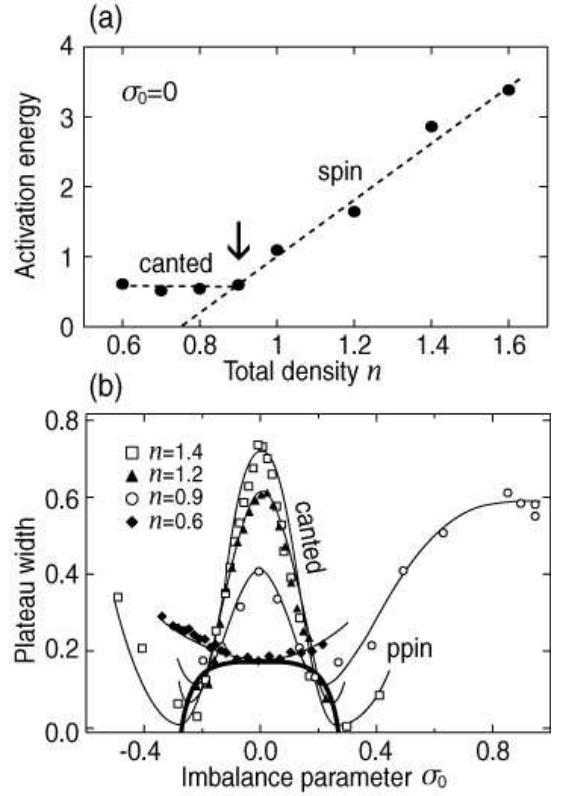

FIG. 8: The activation-energy data for ρ_0 and the plateau-width data for σ_0 are taken from Sawada et al.[7]. In the upper figure (a), the point $n = 0.9$ is identified with the spin-canted phase transition point. In the lower figure (b), the minimum point in each curve indexed by n is identified with the ppin-canted phase transition point. The heavy curve traces these minimum points.

phase diagram for $d/\ell_B = 1.23$ is similar to the one for $d/\ell_B = 1$, it would be allowed to extrapolate the exact diagonalization data from $d/\ell_B = 1$. We have plotted it on the same figure as indicated by the dotted curve [FIG.9]. Then the point is also near to the ppin-canted phase boundary. It is hard to decide on which phase boundary this point exists from this phase diagram.

We answer this problem based on the phase diagram in the σ_0-ρ_0 plane [FIG.6]. We focus on the horizontal line at $n = 0.9$. This corresponds to the curve indexed by $n = 0.9$ in the plateau-width data [FIG.8(b)]. The curve takes a maximum at $\sigma_0 = 0$ and a minimum at $\sigma_0 \simeq 0.2$ as the density imbalance is made. It is reasonable to identify the region $\sigma_0 > 0.2$ with the ppin phase. Then the region $0 < \sigma_0 < 0.2$ must be the canted phase. Note that the spin phase is realized only at $\sigma_0 = 0$. We conclude that the point $(\sigma_0, n) = (0.2, 0.9)$ represents the ppin-canted phase transition point and that the point $(\sigma_0, n) = (0, 0.9)$ found in the activation-energy data represents the spin-canted phase transition [FIG.6]. This interpretation is consistent with the fact that no indication of phase transion is found for $0.9 < n < 1.6$ in the same data [FIG.8(a)].
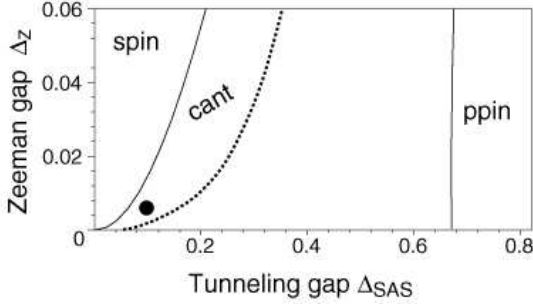
FIG. 9: The phase diagram is given in the Δ_{SAS}-Δ_Z plane for $\Delta_{bias} = 0$ and $d = 1.23\ell_B$. We have taken the Coulomb energy unit E_C^0 for the tunneling gap (horizontal axis) and the Zeeman gap (vertical axis). The large point is the experimental data indicating a phase transition point taken from Sawada et al.[7]. The two solid curves represent the phase boundaries in the first order of perturbation. The dotted curve stands for the ppin-canted phase boundary extrapolated from the exact diagonalization result obtained at $d = \ell_B$ for the 12 electron system[9]. It is hard to decide on which phase boundary this point exists from this phase diagram.

We continue to examine the plateau-width data for the sample with various density n [FIG.8(b)]. The data with $n = 1.4$ and $n = 1.2$ show similar behaviors as the one with $n = 0.9$. Namely, they possess the minimum points to be identified with the ppin-canted phase transitions around the imbalance parameter $\sigma_0 \simeq 0.3$. It is observed that the ppin-canted transition point σ_0 decreases as n decreases. It is not clear from the data when the ppin-canted phase transition disappears as n decreases. However, it seems that the entire region belongs to the ppin phase at $n = 0.6$. Let us tentatively regard the critical point exists near the point $n = 0.6$. In this way we have speculated the real ppin-canted boundary in the phase diagram in the σ_0-ρ_0 plane [FIG.6] and in the ρ_0-Δ_{SAS} plane [FIG.7].

VIII. DISCUSSIONS

There are three phases, i.e., the spin phase, the canted phase and the ppin phase at $\nu = 2$. The ground state is the fully spin polarized state (4.9) in the spin phase, while it is the fully pseudospin polarized state (4.11) in the ppin phase. In the canted phase, however, it is not simply made of a certain combination of these two states, as postulated in a phenomenological bosonic spin model[15], but made of more states in a very complicated way. We have constructed the ground states explicitly in the first order of perturbation.

The phase diagram has been studied numerically within the Hartree-Fock approximation in the standard literature[4,5,8,13]. In this paper we have presented analytic formulas for it based on perturbation theory. Our results in the first order approximation reproduce precisely the Hartree-Fock variational result[13] at the zero bias voltage,

and agree qualitatively with numerical results for nonzero bias voltages[8,13]. We have also argued how the phase diagram is modified by higher order quantum corrections. We have shown that the spin-canted phased boundary is not modified but the ppin-canted phase boundary is considerably modified. It is necessary to develop a reliable theory including higher order quantum corrections to determine the accurate ppin-canted boundary in various phase diagrams.

Our new contribution is the phase diagrams in the σ_0-ρ_0 plane as well as in the Δ_{bias}-ρ_0 plane. We have analyzed the relation between the imbalance parameter σ_0 and the bias voltage V_{bias}. At $\nu = 1$ the density imbalance occurs as soon as the bias voltage becomes nonzero. However, this is not the case at $\nu = 2$ as in FIG.1, where $\Delta_{bias} = eV_{bias}$. As far as $V_{bias} < V_{bias}^{sc}$ the density imbalance is not induced and the system is still in the spin phase. A charge imbalance occurs only above a certain critical value V_{bias}^{sc} of the bias voltage, where the system is driven into the canted phase. As the bias voltage increases above a second critical value V_{bias}^{pc}, the system turns into the ppin phase. Taking these facts into account we have constructed the phase diagram in the σ_0-ρ_0 plane as well as in the Δ_{bias}-ρ_0 plane. These phase diagrams will be useful to identify the three phases experimentally by using a single sample. We have also presented the phase diagram in the ρ_0-Δ_{SAS} plane. It will be useful to identify the three phases experimentally by using several samples with different Δ_{SAS} but all other parameters unchanged.

We have interpreted experimental data due to Sawada et al.[7,14]. We admit that our analysis is far from satisfactory. This is mainly because of the lack of qualified data. Recall that the primary concern of these experiments were to reveal the existence of the interlayer coherent phase at $\nu = 2$, which is identified with the ppin phase in the present terminology. In passing detailed experiments with several samples are urged to be performed in order to establish the ground-state structure in the $\nu = 2$ bilayer QH system.

APPENDIX A: PHYSICAL VARIABLES

The basis of the algebra SU(4) is spanned by 15 Hermitian traceless matrices. For our purposes it is convenient to choose them as $\tau_a^{\rm spin}$, $\tau_a^{\rm ppin}$ and $\tau_a^{\rm spin}\tau_b^{\rm ppin}$ given by

$$\tau_a^{\rm spin} = \begin{pmatrix} \tau_a & 0 \\ 0 & \tau_a \end{pmatrix}, \quad \tau_x^{\rm ppin} = \begin{pmatrix} 0 & \mathbb{I} \\ \mathbb{I} & 0 \end{pmatrix},$$

$$\tau_y^{\rm ppin} = \begin{pmatrix} 0 & -i\mathbb{I} \\ +i\mathbb{I} & 0 \end{pmatrix}, \quad \tau_z^{\rm ppin} = \begin{pmatrix} \mathbb{I} & 0 \\ 0 & -\mathbb{I} \end{pmatrix}, \quad \text{(A1)}$$

where $\mathbb{I}$ denotes the 2×2 identity matrix, and τ_a are the Pauli matrices.

A basis in the space of 4×4 antisymmetric matrices, comprised of 6 matrices, can be chosen as $\tau_a^{\rm spin}\tau_x^{\rm spin}\tau_y^{\rm ppin}$ and $\tau_a^{\rm ppin}\tau_x^{\rm spin}\tau_y^{\rm ppin}$. Hence, introducing four tree-dimensional vectors $\boldsymbol{A}$, $\boldsymbol{B}$, $\boldsymbol{C}$ and $\boldsymbol{D}$, we may parameterize the matrix g as

$$\begin{aligned} 2g =& (A_x + iB_x)\tau_z^{\rm spin}\tau_y^{\rm ppin} + (C_x + iD_x)\tau_y^{\rm spin}\tau_z^{\rm ppin} \\ &+ (A_y + iB_y)(-i\tau_y^{\rm ppin}) + (C_y + iD_y)(-i\tau_y^{\rm spin}) \\ &+ (A_z + iB_z)(-\tau_x^{\rm spin}\tau_y^{\rm ppin}) + (C_z + iD_z)(-\tau_y^{\rm spin}\tau_x^{\rm ppin}) \\ =& -i\left[(\boldsymbol{A} + i\boldsymbol{B})\boldsymbol{\tau}^{\rm spin} + (\boldsymbol{C} + i\boldsymbol{D})\boldsymbol{\tau}^{\rm ppin}\right]\tau_x^{\rm spin}\tau_y^{\rm ppin}. \end{aligned}$$
$$\text{(A2)}$$

We come to

$$\begin{aligned} gg^\dagger =& \frac{1}{4}(\boldsymbol{A}^2 + \boldsymbol{B}^2 + \boldsymbol{C}^2 + \boldsymbol{D}^2) \\ &+ \frac{1}{2}\tau_a^{\rm spin}\varepsilon_{abc}A_bB_c + \frac{1}{2}\tau_a^{\rm ppin}\varepsilon_{abc}C_bD_c \\ &+ \frac{1}{2}\tau_a^{\rm spin}\tau_b^{\rm ppin}(A_aC_b + B_aD_b). \end{aligned} \quad \text{(A3)}$$

Comparing this with (3.11) we get

$$\mathcal{S}_a = \varepsilon_{abc}A_bB_c, \quad \text{(A4a)}$$
$$\mathcal{P}_a = \varepsilon_{abc}C_bD_c, \quad \text{(A4b)}$$
$$\mathcal{R}_{ab} = A_aC_b + B_aD_b, \quad \text{(A4c)}$$

from which we derive the constraints

$$\mathcal{S}_a\mathcal{R}_{ab} = 0, \quad \text{(A5a)}$$
$$\mathcal{R}_{ab}\mathcal{P}_b = 0, \quad \text{(A5b)}$$
$$\mathcal{S}_a\mathcal{P}_b - \varepsilon_{acd}\varepsilon_{bhe}\mathcal{R}_{ch}\mathcal{R}_{de} = 0 \quad \text{(A5c)}$$

on $\mathcal{S}_a$, $\mathcal{P}_a$ and $\mathcal{R}_{ab}$. The constraint (A5c) is verified based on the identity

$$\begin{aligned} \varepsilon_{acd}\varepsilon_{bhe} =& \delta_{ab}\left(\delta_{ch}\delta_{de} - \delta_{ce}\delta_{dh}\right) - \delta_{ah}\left(\delta_{cb}\delta_{de} - \delta_{ce}\delta_{bd}\right) \\ &+ \delta_{ae}\left(\delta_{cb}\delta_{dh} - \delta_{ch}\delta_{bd}\right), \end{aligned} \quad \text{(A6)}$$

while (A4a) and (A4b) trivially follow from (A5a) and (A5b).

We construct $\mathcal{R}_{ab}$ satisfying (A5a)–(A5c). To satisfy the constraint (A5a) we use the two normalized vectors

$$\frac{\boldsymbol{S}^2\mathcal{P}_a - (\boldsymbol{S}\boldsymbol{P})\mathcal{S}_a}{\mathcal{S}\mathcal{Q}}, \qquad \frac{\mathcal{Q}_a}{\mathcal{Q}}, \quad \text{(A7)}$$

which are orthogonal to $\mathcal{S}_a$, and orthogonal one to another. To satisfy the constraint (A5b) we use the two normalized vectors

$$\frac{\boldsymbol{P}^2\mathcal{S}_b - (\boldsymbol{S}\boldsymbol{P})\mathcal{P}_b}{\mathcal{P}\mathcal{Q}}, \qquad \frac{\mathcal{Q}_b}{\mathcal{Q}}, \quad \text{(A8)}$$

which are orthogonal to $\mathcal{P}_b$, and orthogonal one to another. Hence we are able to expand $\mathcal{R}_{ab}$ in terms of 4 tensors made out of these vectors with 4 coefficients $\mathcal{R}_{PS}$, $\mathcal{R}_{PQ}$, $\mathcal{R}_{QS}$ and $\mathcal{R}_{QQ}$ as in (3.25) in text. We now substitute (3.25) into the constraint (A5c) to find that

$$\mathcal{R}_{QS}\mathcal{R}_{PQ} - \mathcal{R}_{PS}\mathcal{R}_{QQ} = \boldsymbol{S}\boldsymbol{P}. \quad \text{(A9)}$$

Consequently three variables are independent among $\mathcal{R}_{PS}$, $\mathcal{R}_{PQ}$, $\mathcal{R}_{QS}$ and $\mathcal{R}_{QQ}$. They are parametrized as in (3.26).

APPENDIX B: UNPHYSICAL VARIABLES

We have identified 9 independent physical variables in the 12 parameters of the antisymmetric matrix g. In this appendix we identify the 3 unphysical variables. In so doing we derive the kinematical condition (3.17), i.e., $\boldsymbol{S}^2 + \boldsymbol{P}^2 + \boldsymbol{R}^2 \leq 1$.

The matrix g is expanded in terms of 4 three-dimensional vectors $\boldsymbol{A}$, $\boldsymbol{B}$, $\boldsymbol{C}$ and $\boldsymbol{D}$ as in (A2). We investigate how they are given in terms of the physical variables. For this purpose we reverse the constraints (A4a) and (A4b). The most general expressions read

$$\begin{aligned} A_a =& \frac{\boldsymbol{S}^2\mathcal{P}_a - (\boldsymbol{S}\boldsymbol{P})\mathcal{S}_a}{\mathcal{S}\mathcal{Q}}\theta_A + \frac{\mathcal{Q}_a}{\mathcal{Q}}\zeta_A, \\ B_a =& \frac{\boldsymbol{S}^2\mathcal{P}_a - (\boldsymbol{S}\boldsymbol{P})\mathcal{S}_a}{\mathcal{S}\mathcal{Q}}\theta_B + \frac{\mathcal{Q}_a}{\mathcal{Q}}\zeta_B, \\ C_a =& \frac{\boldsymbol{P}^2\mathcal{S}_a - (\boldsymbol{S}\boldsymbol{P})\mathcal{P}_a}{\mathcal{P}\mathcal{Q}}\theta_C + \frac{\mathcal{Q}_a}{\mathcal{Q}}\zeta_C, \\ D_a =& \frac{\boldsymbol{P}^2\mathcal{S}_a - (\boldsymbol{S}\boldsymbol{P})\mathcal{P}_a}{\mathcal{P}\mathcal{Q}}\theta_D + \frac{\mathcal{Q}_a}{\mathcal{Q}}\zeta_D, \end{aligned} \quad \text{(B1)}$$

where the parameters $\theta_{A,B}$ and $\zeta_{A,B}$ are restricted by

$$\theta_A\zeta_B - \zeta_A\theta_B = \mathcal{S}, \quad \text{(B2)}$$
$$\theta_D\zeta_C - \zeta_D\theta_C = \mathcal{P}. \quad \text{(B3)}$$

We substitute (B1) into (A4c), and compare the resulting equation with (3.25). In this way we obtain new restrictions,

$$\begin{bmatrix} \theta_A & \theta_B \\ \zeta_A & \zeta_B \end{bmatrix}\begin{bmatrix} \theta_C \\ \theta_D \end{bmatrix} = \begin{bmatrix} \mathcal{R}_{PS} \\ \mathcal{R}_{QS} \end{bmatrix},$$
$$\begin{bmatrix} \theta_A & \theta_B \\ \zeta_A & \zeta_B \end{bmatrix}\begin{bmatrix} \zeta_C \\ \zeta_D \end{bmatrix} = \begin{bmatrix} \mathcal{R}_{PQ} \\ \mathcal{R}_{QQ} \end{bmatrix}. \quad \text{(B4)}$$

We solve these as

$$\theta_C = \frac{\mathcal{R}_{PS}\zeta_B - \mathcal{R}_{QS}\theta_B}{\mathcal{S}}, \quad \theta_D = \frac{\mathcal{R}_{QS}\theta_A - \mathcal{R}_{PS}\zeta_A}{\mathcal{S}},$$
$$\zeta_C = \frac{\mathcal{R}_{PQ}\zeta_B - \mathcal{R}_{QQ}\theta_B}{\mathcal{S}}, \quad \zeta_D = \frac{\mathcal{R}_{QQ}\theta_A - \mathcal{R}_{PQ}\zeta_A}{\mathcal{S}}.$$
$$(B5)$$

It is trivial to check that (B3) is automatically satisfied due to (A9) and (B2). We count the number of independent variables. There are 9 physical variables; $\mathcal{S}_a$, $\mathcal{P}_a$, $\mathcal{R}_{PS}$, $\mathcal{R}_{PQ}$, $\mathcal{R}_{QS}$ and $\mathcal{R}_{QQ}$ with one constraint (A9). There are 3 extra variables; θ_A, θ_B, ζ_A and ζ_B with one constraint (B2). We now show that they are the unphysical variables.

A well-known unphysical variable is the overall phase of the ground state. First we identify it. We consider two vectors (θ_A, θ_B) and (ζ_A, ζ_B). We rotate the two vectors (θ_A, θ_B) and (ζ_A, ζ_B) by a single angle ϕ, which is the overall angle common to them. It turns out that the two vectors (θ_C, θ_D) and (ζ_C, ζ_D) rotate by the same angle due to (B5). Then, (A_a, B_a) and (C_a, D_a) rotate in the same way due to (A5b). Finally, (A2) implies that the matrix g acquires the angle ϕ, which is the overall phase of the ground state.

Another well-known unphysical variable is associated with the normalization of the ground state. The normalization condition (3.3) is equivalent to

$$\boldsymbol{A}^2 + \boldsymbol{B}^2 + \boldsymbol{C}^2 + \boldsymbol{D}^2 = 2. \tag{B6}$$

Substituting (B1) into this and using (B5), we obtain

$$\begin{aligned} \mathcal{S}^2 = &\frac{1}{2}\left(\theta_A^2 + \theta_B^2\right)\left(\mathcal{S}^2 + \mathcal{R}_{QS}^2 + \mathcal{R}_{QQ}^2\right) \\ &+ \frac{1}{2}\left(\zeta_A^2 + \zeta_B^2\right)\left(\mathcal{S}^2 + \mathcal{R}_{PS}^2 + \mathcal{R}_{PQ}^2\right) \\ &- \left(\theta_A\zeta_A + \theta_B\zeta_B\right)\left(\mathcal{R}_{QS}\mathcal{R}_{PS} + \mathcal{R}_{QQ}\mathcal{R}_{PQ}\right). \end{aligned} \tag{B7}$$

We make a change of variables. Let γ be the angle between the vectors (θ_A, θ_B) and (ζ_A, ζ_B). Omitting the overall angle we may write

$$(\theta_A, \theta_B) = \left(\theta\cos\frac{\gamma}{2}, -\theta\sin\frac{\gamma}{2}\right),$$
$$(\zeta_A, \zeta_B) = \left(\zeta\cos\frac{\gamma}{2}, \zeta\sin\frac{\gamma}{2}\right). \tag{B8}$$

Next, we introduce new variables x and y by

$$x = \theta^2\left[1 + \frac{\mathcal{R}_{QS}^2 + \mathcal{R}_{QQ}^2}{\mathcal{S}^2}\right] + \zeta^2\left[1 + \frac{\mathcal{R}_{PS}^2 + \mathcal{R}_{PQ}^2}{\mathcal{S}^2}\right],$$
$$y = \theta^2\left[1 + \frac{\mathcal{R}_{QS}^2 + \mathcal{R}_{QQ}^2}{\mathcal{S}^2}\right] - \zeta^2\left[1 + \frac{\mathcal{R}_{PS}^2 + \mathcal{R}_{PQ}^2}{\mathcal{S}^2}\right],$$
$$(B9)$$

which we use instead of θ^2 and ζ^2. Now, there are three variables x, y and γ with two constraints (B2) and (B7).

We denote

$$a = \frac{\mathcal{S}^2\left(\mathcal{S}^2 + \mathcal{P}^2 + \mathcal{R}^2\right)}{\left(\mathcal{S}^2 + \mathcal{R}_{QS}^2 + \mathcal{R}_{QQ}^2\right)\left(\mathcal{S}^2 + \mathcal{R}_{PS}^2 + \mathcal{R}_{PQ}^2\right)}, \tag{B10}$$

or

$$\frac{a}{1-a} = \frac{\mathcal{S}^2\left(\mathcal{S}^2 + \mathcal{P}^2 + \mathcal{R}^2\right)}{(\mathcal{R}_{QS}\mathcal{R}_{PS} + \mathcal{R}_{QQ}\mathcal{R}_{PQ})^2}. \tag{B11}$$

Here

$$\mathcal{R}^2 \equiv \mathcal{R}_{ab}^2 = \mathcal{R}_{PS}^2 + \mathcal{R}_{PQ}^2 + \mathcal{R}_{QS}^2 + \mathcal{R}_{QQ}^2, \tag{B12}$$

where the last equality follows from (3.25).

Using the above notations two constraints (B2) and (B7) are rearranged into

$$\cos\gamma = \frac{x-2}{\sqrt{(1-a)(x^2-y^2)}},$$
$$\sin\gamma = \frac{2\sqrt{\mathcal{S}^2 + \mathcal{P}^2 + \mathcal{R}^2}}{\sqrt{a(x^2-y^2)}}. \tag{B13}$$

These are well defined since $x^2 > y^2$ and $0 < a < 1$, as follows from definitions (B9) and (B10). It follows that

$$\frac{(x-2)^2}{(1-a)(x^2-y^2)} + \frac{4(\mathcal{S}^2 + \mathcal{P}^2 + \mathcal{R}^2)}{a(x^2-y^2)} = 1 \tag{B14}$$

from $\cos^2\gamma + \sin^2\gamma = 1$, or

$$(ax - 2)^2 + a\left(1-a\right)y^2 = 4\left(1-a\right)\left(1 - \mathcal{S}^2 - \mathcal{P}^2 - \mathcal{R}^2\right). \tag{B15}$$

We ask the question whether (B15) admits solutions for x and y which leads to positive values of θ^2 and ζ^2 via (B9). The solvability condition turns out to be

$$\mathcal{S}_a^2 + \mathcal{P}_a^2 + \mathcal{R}_{ab}^2 \leqslant 1. \tag{B16}$$

This is the condition (3.17) for the magnitude of the isospin.

If the condition is satisfied, we may solve x and y from (B15), and obtain θ, ζ and γ from (B9) and (B13). Solutions are not unique. Eq.(B15) defines an ellipse. Moving along the ellipse the parameters θ, ζ and γ take different values, and therefore lead to different vectors $\boldsymbol{A}$, $\boldsymbol{B}$, $\boldsymbol{C}$ and $\boldsymbol{D}$. However, all these vectors lead to one and the same set of physical fields $\mathcal{S}_a$, $\mathcal{P}_a$ and $\mathcal{R}_{ab}$. This is the unphysical variable inherent to the $\nu = 2$ bilayer QH system, which is commented below (3.26). This unphysical mode decouples on the ground state since the ellipse is shrunk to a point, as we see in the following appendix.

APPENDIX C: GROUND-STATE CONDITION

The eigenvalue equation (3.5) in the SU(4)-invariant system leads to the condition (3.13), or

$$\epsilon_{\alpha\beta\mu\nu}g_{\alpha\beta}g_{\mu\nu} = 0. \tag{C1}$$

On the other hand, the variational ground state in the full SU(4)-noninvariant system is found to satisfy (3.14), or

$$\boldsymbol{S}^2 + \boldsymbol{P}^2 + \boldsymbol{R}^2 = 1. \tag{C2}$$

We verify the equivalence of these two conditions.

For this purpose, we substitute (A2) into (C1), and use (B6), to obtain

$$\boldsymbol{A}^2 + \boldsymbol{D}^2 = \boldsymbol{B}^2 + \boldsymbol{C}^2 = 1, \quad \boldsymbol{A}\boldsymbol{B} = \boldsymbol{C}\boldsymbol{D}. \tag{C3}$$

On the other hand, examining this step of transformation we see that (C1) follows from (C3). Namely, (C1) is equivalent to (C3) based on the formula (A2).

The derivation of (C2) from (C3) is easy. Using (A4) we express $\boldsymbol{S}^2 + \boldsymbol{P}^2 + \boldsymbol{R}^2$ in terms of $\boldsymbol{A}$, $\boldsymbol{B}$, $\boldsymbol{C}$ and $\boldsymbol{D}$. We then use (C3) to derive (C2).

The derivation of (C3) from (C2) is more complicated. When the condition (C2) holds, the ellipse defined by (B15) is shrunk to a point set given by $ax = 2$ and $y = 0$. In this case, θ and ζ are determined by solving (B9),

$$\theta = \sqrt{\mathcal{S}^2 + \mathcal{R}_{PS}^2 + {}_{PQ}^2}, \quad \zeta = \sqrt{\mathcal{S}^2 + \mathcal{R}_{QS}^2 + \mathcal{R}_{QQ}^2}, \tag{C4}$$

and (B13) becomes

$$\cos\gamma = \sqrt{1-a}, \qquad \sin\gamma = \sqrt{a}, \tag{C5}$$

where a is given by (B10). First we note that

$$\boldsymbol{A}^2 + \boldsymbol{D}^2 = \theta_A^2 + \zeta_A^2 + \theta_D^2 + \zeta_D^2, \tag{C6}$$

to which we substitute (B5) and (B8). We then use (B7), (C4) and (C5). In this way we prove $\boldsymbol{A}^2 + \boldsymbol{D}^2 = 1$ after some straightforward calculation. Similarly we can verify all equations in (C3).

As we have seen, the unphysical variables θ, ζ and γ are fixed in terms of the physical variables on the ground state, where the condition (C2) is satisfied. Thus, every ground-state configuration has a unique matrix $g_{\mu\nu}$. We substitute (3.26), (3.34) and (3.36c) into (C4) and (C5). Choosing $\omega = \pi/4$, for simplicity, we find

$$\theta = \zeta = \frac{\sqrt{\Delta_0^2 + \Delta_Z^2\left(1-\beta^2\right)}}{\Delta_0}\sqrt{1-\alpha^2}, \tag{C7}$$

and

$$
\begin{aligned}
\cos\frac{\gamma}{2} &= \frac{\Delta_0}{\sqrt{\Delta_0^2 + \Delta_Z^2\left(1-\beta^2\right)}}, \\
\sin\frac{\gamma}{2} &= \frac{\Delta_Z\sqrt{1-\beta^2}}{\sqrt{\Delta_0^2 + \Delta_Z^2\left(1-\beta^2\right)}}.
\end{aligned}
\tag{C8}
$$

Using (C7) and (C8) in (B8) we obtain

$$
\begin{aligned}
\theta_A &= \zeta_A = \sqrt{1-\alpha^2}, \\
\theta_B &= -\zeta_B = -\frac{\Delta_Z}{\Delta_0}\sqrt{1-\alpha^2}\sqrt{1-\beta^2}.
\end{aligned}
\tag{C9}
$$

Now, it is straightforward to express $\boldsymbol{A}$, $\boldsymbol{B}$, $\boldsymbol{C}$ and $\boldsymbol{D}$ in terms of α and β, and hence to reconstruct the matrix $g_{\mu\nu}$ as in (4.4).

[1] Z.F. Ezawa, *Quantum Hall Effects: Field Theoretical Approach and Related Topics* (World Scientific, 2000).

[2] S. Das Sarma and A. Pinczuk (eds), *Perspectives in Quantum Hall Effects* (Wiley, 1997).

[3] In the standard literature the spin-ferromagnet and pseudospin-singlet phase is called the ferromagnet phase, while the spin-singlet and pseudospin-ferromagnet phase is called the singlet phase. Here, we call them the spin phase and the ppin phase to respect their equal partnership.

[4] L. Zheng, R.J. Radtke and S. Das Sarma, Phys. Rev. Lett. 78 (1997) 2453.

[5] S. Das Sarma, S. Sachdev and L. Zheng, Phys. Rev. Lett. 79 (1997) 917; Phys. Rev. B58 (1998) 4672.

[6] V. Pellegrini, A. Pinczuk, B.S. Dennis, A.S. Plaut, L.N. Pfeiffer and K.W. West, Phys. Rev. Lett. 78 (1997) 310; Science 281 (1998) 799.

[7] A. Sawada, Z.F. Ezawa, H. Ohno, Y. Horikoshi, Y. Ohno, S. Kishimoto, F. Matsukura, M. Yasumoto and A. Urayama Phys. Rev. Lett. 80 (1998) 4534.

[8] L. Brey, E. Demler and S. Das Sarma, Phys. Rev. Lett. 83 (1999) 168.

[9] J. Schliemann and A.H. MacDonald, Phys. Rev. Lett. 84 (2000) 4437.

[10] Z.F. Ezawa and G. Tsitsishvili, Phys. Rev. B70 (2004) 125304.

[11] K. Hasebe and Z.F. Ezawa, Phys. Rev. B66 (2002) 155318.

[12] Z.F. Ezawa, G. Tsitsishvili and K. Hasebe, Phys. Rev. B67 (2003) 125314.

[13] A.H. MacDonald, R. Rajaraman and T. Jungwirth, Phys. Rev. B60 (1999) 8817.

[14] A. Sawada, Z.F. Ezawa, H. Ohno, Y. Horikoshi, A. Urayama, Y. Ohno, S. Kishimoto, F. Matsukura and N. Kumada, Phys. Rev. B59 (1999) 14888.

[15] E. Demler and S. Das Sarma, Phys. Rev. Lett. 82 (1999) 3895.